frontiers in Earth Science

ORIGINAL RESEARCH
published: 03 May 2019
doi: 10.3389/feart.2019.00087

Increased Stability in Carbon Isotope Records Reflects Emerging Complexity of the Biosphere

Martin Schobben and Bas van de Schootbrugge*

Department of Earth Sciences, Utrecht University, Utrecht, Netherlands

Preference for certain stable isotopes (isotope fractionation) during enzyme-mediated reactions is a universal aspect of life. For instance, carbon isotopes are fractionated during anabolic (e.g., photosynthate production) and catabolic (e.g., methanogenesis) reactions. These biological processes exert a major control on ambient micro-scale chemical conditions as well as the large-scale exogenic carbon reservoir. Combined with the ubiquity of bio-mediated carbonate mineral nucleation and obligate enzymatic skeletonization, these biochemical reactions and their control on the exogenic carbon pool are known to leave distinct imprints on carbonate minerals which accumulate as sediments throughout Earth's history. Here, we study the evolution of the marine carbonate-carbon isotope record based on database compilations from the Precambrian and the Phanerozoic. By looking at the frequency distribution of the amplitude of stratigraphic variation at various temporal resolutions, we assess trends in the carbonate-carbon isotope variability. Part of this variation can only be explained by authigenic and diagenetic carbonate mineral additions, which carry metabolic carbon isotope signatures created in the vicinity of cells and secluded (sub-)seafloor micro-environments. It can be envisioned that compartmentalization (membrane enclosed regions), the accumulation of extracellular polymeric substances (biofilms), and restricted fluid exchange in the early diagenetic environment can create sharp isotope gradients that lead to a high-order of micro-scale carbon isotope variability being imprinted in carbonate rock. The frequency of the high-amplitude variation diminishes with the development of more complex life (metazoan-dominated biosphere); presumably through the dispersing action of bioturbation (eradicating these micro-environments), increased grazing pressure and the advent of obligate biomineralization. On the other hand, stark chemical gradients in a world dominated by unicellular life (prokaryotes and to a lesser extent eukaryotes) are thought to leave a distinctly more variable C isotope signature in carbonate rock. An enhanced understanding of the biogenicity of carbonate carbon isotope signatures at multiple spatial and temporal scales provides a baseline that is usable in the search for signs of (past) extraterrestrial life.

Keywords: carbon cycle, microbial carbonate, diagenesis, biosignatures, bioturbation, evolutionary innovation, biofilms, biomineralization

OPEN ACCESS

Edited by:
Mónica Sánchez-Román, Vrije Universiteit Amsterdam, Netherlands

Reviewed by:
Karim Benzerara, Centre National de la Recherche Scientifique (CNRS), France
Linda C. Kah, The University of Tennessee, Knoxville, United States
Joshua Erik Krissansen-Totton, University of Washington, United States

****Correspondence:***
Martin Schobben
m.a.n.schobben@uu.nl

Specialty section:
This article was submitted to Microbiological Chemistry and Geomicrobiology, a section of the journal Frontiers in Earth Science

Received: *03 October 2018*
Accepted: *08 April 2019*
Published: *03 May 2019*

Citation:
Schobben M and van de Schootbrugge B (2019) Increased Stability in Carbon Isotope Records Reflects Emerging Complexity of the Biosphere. Front. Earth Sci. 7:87. doi: 10.3389/feart.2019.00087

INTRODUCTION

Global marine deposits of carbonate minerals constitute the largest archive of past and present activity by life on Earth (Skinner and Jahren, 2003). Although carbonate precipitation can occur purely abiotically (Arp et al., 1999; Ridgwell, 2005), in today's oceans; foraminifera, coccolithophorids and pteropods in the open ocean, and corals and mollusks in shallow-water environments, are responsible for virtually all carbonate production (Knoll, 2003; Skinner and Jahren, 2003; Sarmiento and Gruber, 2004). The connection between organisms and carbonate deposits becomes more obscure with increasing age, as skeletonized parts become scarce prior to the Cambrian (Grant, 1990; Grotzinger et al., 1995, 2000; Knoll and Carroll, 1999; Valentine et al., 1999; Wood et al., 2002; Knoll, 2003; Porter, 2010; Darroch et al., 2018; Mehra and Maloof, 2018; Vaziri et al., 2018). It thus follows, that large portions of the carbonate archive were produced by a different carbonate factory.

Many microbes (bacteria and archaea) may induce precipitation of carbonate minerals in the immediate vicinity of their cells as a side product of their metabolic activity (Pentecost and Spiro, 1990; Merz, 1992; McConnaughey and Whelan, 1997; Dupraz and Visscher, 2005; Visscher and Stolz, 2005). These bio-mediated carbonate precipitates can form within the water column, on the seafloor, and potentially deep underground within pore spaces of buried sediments; and they accumulate in marine sedimentary stacks that form in a broad spectrum of environments, ranging from the deep sea to the intertidal zone (Webb, 1996; Riding, 2000; Mackenzie and Andersson, 2011). Precipitation of carbonate minerals in the presence of microbes is thought to be triggered by changes in the inorganic carbonate chemistry through organic matter decay and enzymatic reactions (e.g., carbon fixation by carbonic anhydrase) (Pentecost and Spiro, 1990; Merz, 1992; Thompson and Ferris, 1992; Pentecost and Franke, 2010; Bundeleva et al., 2014), or by overcoming energetic barriers through the removal of surface inhibitors (e.g., magnesium and phosphate) and the growth of organic templates (Reitner, 1993; Vasconcelos et al., 1995; Arp et al., 2003). Field observations in modern aquatic environments have had a large focus on bio-mediated carbonate precipitation within dense microbial mats consisting of stratified layers of exopolymeric substances (EPS) that host a range of microbes from different metabolic groups (e.g., oxygenic photosynthesizers and anaerobic heterotrophs) (Visscher et al., 2000; Dupraz and Visscher, 2005; Visscher and Stolz, 2005; Glunk et al., 2010). Laboratory experiments on cultures of cyanobacteria as well as members of aerobic and anaerobic bacteria have generated several species-specific models of bio-mediated carbonate precipitation, which implicate the combined action of metal ion adsorption (Ca^{2+}, Mg^{2+}, and Fe^{2+}) on microbial cell surfaces (and EPS) and alkalinization of the extracellular fluid by metabolic activity, and thereby locally change the saturation state in favor of carbonate mineral precipitation (Sánchez-Román et al., 2008, 2014; Bundeleva et al., 2014).

The literature and nomenclature on bio-mediated carbonate precipitates is vast, and terms like; "microbially controlled, -mediated, –induced and -influenced," are often used to reflect the degree of control of the organism over precipitation. In this study, we restrict ourselves to one term: "bio-mediated carbonate precipitation." This is based on the notion that these bio-mediated reactions are distinct from the metabolically costly process of "enzymatic skeletonization," where nucleation, crystal growth and termination is actively controlled by ion transport across membranes, intracellular vesicles, and organic templates. The hard parts produced by this enzymatic process provide mechanical properties beneficial for the survival of the organism (e.g., protection and structure) (Marin et al., 1996, 2000; McConnaughey and Whelan, 1997; Vermeij, 1977; Westbroek and Marin, 1998; Knoll, 2003). Nonetheless, certain forms of bio-mediated carbonate precipitation appear to be more intimately connected with the organism's physiology; e.g., carbonate nucleation by cyanobacteria could be beneficial for the cell-internal proton balance (McConnaughey and Whelan, 1997). Combined with the observation that cell-internal calcification might exist in some cyanobacteria species, and the frequent independent appearance of enzymatic skeletonization in the evolutionary history of life (Merz, 1992; McConnaughey and Whelan, 1997; Knoll, 2003; Pentecost and Franke, 2010; Benzerara et al., 2014), this notion supports our conservative classification into "bio-mediated carbonate precipitation" and "enzymatic skeletonization" as end-members for a Precambrian prokaryote-, and a Phanerozoic metazoan-dominated biosphere on a broad spectrum of possible calcification pathways.

By contrast to the relatively young fossil record of enzymatic skeletonization, palaeontological evidence of bio-mediated carbonate precipitates is arguably as old as ∼3,800–3,500 Ma (Archaean), and points to the antiquity of this type of biological control on carbonate deposition (Allwood et al., 2006; Lepot et al., 2008; Nutman et al., 2016). Both macroscopic sedimentary structures known as microbialites (e.g., mounds, thrombolites, and stromatolites) and sedimentary textures (e.g., tufa, peloids, and fenestra) have been classified as ancient bio-mediated carbonate precipitates (Pope and Grotzinger, 2000; Riding, 2000). The most iconic are the stromatolites, commonly viewed as the lithified remnants of microbial mats, and with potential modern analogs in Shark Bay (Western Australia) and Highborne Cay (Bahamas) (Arp et al., 2001; Dupraz and Visscher, 2005; Andres et al., 2006). However, the extent of biological control on the precipitation of some of these old carbonate structures and textures has been questioned, where structures either consist of sediment particles trapped by microbial mats, and others might lack any interference by microbes at all (Grotzinger and Rothman, 1996; Grotzinger and Knoll, 1999; Pope and Grotzinger, 2000; McLoughlin et al., 2008; Allwood et al., 2018). On the other hand, field observations and culture experiments suggest that some bio-mediated carbonate precipitates may be merely pore-occluding diagenetic cements and small aggregates (Folk, 1993; Vasconcelos et al., 1995; Webb, 1996; Sánchez-Román et al., 2008), which could easily go undetected in the rock record with conventional methods (i.e., descriptive sedimentology and petrography). Combined with the notion that calcification seems to intrinsically link

to certain physiologies (McConnaughey and Whelan, 1997), these cryptic bio-mediated carbonate precipitates might be of more widespread importance in both space and time than often assumed.

Geochemical techniques offer an alternative means to determine the link of carbonate mineral deposits with (cryptic) bio-mediated carbonate precipitation. Enrichment patterns of certain trace elements and isotopes in the crystal lattice are connected to microbial activity, which affected the ambient micro-environment of carbonate precipitation (e.g., Andres et al., 2006; Heindel et al., 2012; Birgel et al., 2015; Sforna et al., 2017). The lack of physiological control on bio-mediated carbonate precipitation can be envisioned to result in carbonate mineral assemblages with a heterogeneous chemical composition forced by a range of metabolisms and microhabitats as well as gradients in solutes, metal cycling and high organic carbon (OC) turnover rates in microbial mats and (sub-)seafloor environments (Blair et al., 1985; Merz, 1992; Des Marais and Canfield, 1994; Arp et al., 1999, 2001; Visscher and Stolz, 2005; Andres et al., 2006; Fike et al., 2008; Sforna et al., 2017). On the other hand, variation in the physiological control on bio-mediated carbonate precipitates can result in chemical signatures that directly record the extracellular environment, or more passively reflect the physiologically altered (sub-)seafloor micro-environments that host the organism (Irwin et al., 1977; Mackenzie and Andersson, 2011; Birgel et al., 2015; Schobben et al., 2017).

Carbon isotope composition of bulk carbonate and calcareous skeletons is used to trace variation in the oceanic dissolved inorganic carbon (DIC)-C isotope composition, where fluctuations are dictated by the fluxes in- (weathering, metamorphism and volcanic C) and out (C burial) of the system on geological timescales (>100 ky) (Kump, 1991; Dickens et al., 1995; Kump and Arthur, 1999; Veizer et al., 1999; Zachos et al., 2001; Prokoph et al., 2008). Enzyme-mediated reactions induce carbon isotope fractionations, where the usage of the light ^{12}C isotope is energetically more-favorable during carbon fixation (O'Leary, 1988; Farquhar et al., 1989), leaving the residual DIC pool more-enriched in the ^{13}C isotope. On long geological timescales (>100 ky) a surplus (or deficient) burial of OC can drive the DIC-C isotope composition of the ocean to higher (or lower) values, which is passively imprinted in bulk carbonate and calcareous skeletons as large-scale stratigraphic carbon isotope trends (Garrels and Lerman, 1981; Kump, 1989, 1991; Kump and Arthur, 1999; Veizer et al., 1999). By contrast, in the confined spaces close to the filaments of cyanobacteria ^{13}C-enriched fluids associated with photosynthesis are more directly recorded in carbonate minerals formed by simultaneous bio-mediated carbonate precipitation (Pentecost and Spiro, 1990; Merz, 1992; Schidlowski et al., 1994; Guo et al., 1996). Reversely, the oxidation of reduced carbon (OC and CH_4) introduces again ^{12}C-enriched carbon to the DIC pool, and can as well be recorded by bio-mediated carbonate precipitates as a direct snapshot of the ambient chemical state (Reitner et al., 2005; Andres et al., 2006; Vasconcelos et al., 2006; Meister, 2013). There are two important modes by which these metabolic carbon isotope signatures incorporate into the sediment stack; (1) as ongoing dissolution–recrystallization of metastable primary carbonate precipitates with depth after burial (also known as early diagenesis), where both reactions operate in more-or-less equilibrium (Busenberg and Plummer, 1989; Fantle and DePaolo, 2006, 2007; Mackenzie and Andersson, 2011), and (2) as authigenic carbonate additions which can be regarded as encrusting and void-filling precipitates, where precipitation dominates the reaction balance (Reitner, 1993; Schidlowski et al., 1994; Webb, 1996; Riding, 2000). Both processes of metabolic carbon isotope imprinting on carbonate rock can be envisioned to have been controlled to varying extents by microbes inhabiting the seafloor and sediment. This can either occur directly by providing sites of nucleation on organic templates and alkalinization of fluids in the vicinity of cells (e.g., Sánchez-Román et al., 2008, 2014), or more indirectly by changing the chemical conditions (e.g., pH, total alkalinity and DIC) of porewater in the sediments where exchange with seawater is restricted (Berner et al., 1970; Irwin et al., 1977; Mackenzie and Andersson, 2011; Schrag et al., 2013; Cui et al., 2017; Schobben et al., 2017). Hence, such carbonate carbon isotope signatures have been employed to make inferences about the microbes and metabolism associated within bio-mediated carbonate precipitates of modern environments and ancient rock samples (e.g., Irwin et al., 1977; Andres et al., 2006; Heindel et al., 2012, 2013; Meister, 2013; Birgel et al., 2015).

Metabolic carbon isotope signatures in (especially cryptic) bio-mediated carbonate precipitates might be a more prevalent component of conventional deep time bulk rock-based carbon isotope records than often acknowledged (Knauth and Kennedy, 2009; Schrag et al., 2013; Schobben et al., 2016; Cui et al., 2017). Metabolic carbon isotope signatures will, however, be dampened during the incorporation in the sediment stack by ongoing dissolution–recrystallization reactions and as respiratory carbon mixes with DIC derived from seawater (Schobben et al., 2017). More so, independent constraints on ancient marine chemistry are often lacking. Fortunately, bio-mediated carbonate precipitates might be signified by inherently more spatial heterogeneity (see above), which can be further modulated as a function of the intensity of sediment reworking by biota and grazing of microbial mats. This should result in a more spatially and temporally variable bulk-rock carbon isotope record with shifts at confined stratigraphic scales superimposed on long-term (>100 ky) trends driven by the carbon cycle (Schobben et al., 2017). Here, we examine how predominant such stratigraphic-confined (<100 ky) metabolic carbon isotope signatures are in Earth's carbonate archive throughout different stages of Earth's history. We use database compilations to explore in which ways the amplitude and frequency of small-scale stratigraphic carbon isotope variation changed in conjunction with the development of Earth's biosphere. By separating carbon isotope signatures forced by the global carbon cycle from metabolic carbon isotope signals, our approach will provide a baseline which can be employed to determine the biogenicity of carbonate mineral deposits on Earth and elsewhere in the universe.

MATERIALS AND METHODS

Isotope Notation

Absolute variation in the abundance of the heavy ^{13}C is not easy to measure; as such the ratio of the heavy and light isotope ($^{13}C/^{12}C$) is obtained by isotope ratio mass spectrometry. Subsequently these molar abundance ratios (R_x) are reported relative to a known reference material (R_s) in the delta notation (δ) as 'parts per thousand' (‰),

$$\delta_x = \left(\frac{R_x}{R_s} - 1\right) \times 1000 \quad (1)$$

The data used in this study is sometimes reported against the reference standard PDB (Pee Dee Belemnite), whereas younger studies used today's VPDB (Vienna PDB)-scale, calibrated against the certified reference NBS 19. Values from both scales are virtually identical, and carbon isotope measurements have had a precision of better than 0.1‰ (2*sd*) over the last decades. We use subscripts to denote the material or compositional deviations (e.g., carb is bulk carbonate rock). The main interest of this study is the sample-to-sample $\delta^{13}C_{carb}$ differences from studies on a single stratigraphic sequence (outcrops or cores),

$$\Delta^{13}C_{bed-to-bed} = \delta^{13}C_{upper-bed} - \delta^{13}C_{lower-bed} \quad (2)$$

where the $\Delta^{13}C_{bed-to-bed}$ denotes the $\delta^{13}C_{carb}$ compositional difference of a limestone bed (or layer) relative to the underlying bed. By application of this approach, we attempt to filter-out $\delta^{13}C_{carb}$ oscillations driven by the carbon cycle from published carbon isotope data-sets, with the notion that metabolic carbon isotope signatures are superimposed on these long-term trends as stratigraphic-confined C isotope shifts (i.e., bed-to-bed).

Data Collection

Published bulk-rock carbon isotope data has been collected for four different time windows; (1) the Neogene–Quaternary, (2) the Permian–Triassic, (3) the Ediacaran, and (4) some of the oldest known records that span a long interval of the Precambrian. As a first selection criterion, we circumvented inclusion of $\delta^{13}C_{carb}$ that has been equilibrated in the presence of terrestrial-derived OC in the meteorically influenced diagenetic zone. Decay of this terrestrial OC leads to ^{13}C-depleted DIC being incorporated in cements and replacive carbonate minerals, as a de facto "metabolic signature" under our definition (Brand and Veizer, 1981; Knauth and Kennedy, 2009). Meteorically driven diagenesis is a prevalent feature of Quaternary platform and periplatform carbonate and has been related to high amplitude sea level changes during glacial-interglacial cycles (Melim et al., 2002; Swart, 2008), whereas such differential diagenetic impact on shallow versus pelagic carbonate $\delta^{13}C$ seems absent during greenhouse intervals (Bachan et al., 2017). In our attempt to establish a baseline to evaluate the metabolic imprint of carbonate in relation to a prokaryote- and metazoan-dominated world, the dependence on climatic forcing of meteoric diagenesis, could add substantially more noise to the $\Delta^{13}C_{bed-to-bed}$ record, and is therefore avoided. The latter criterion is, however, constrained to our current state of knowledge on deep time climate.

Neogene and Quaternary bulk-carbonate $\delta^{13}C$ values are from deep water Ocean Drilling Program (ODP) study sites (see the **Supplementary Information** files for sources). By selecting data from these pelagic drill sites we avoid records that could be influenced by meteoric diagenesis. The selection of deep water sites is also favored as these records are less-prone to encompass large sedimentary breaks (Sommerfield, 2006). As a last step, we divided sites of the Neogene–Quaternary time bin according to water depth (above or below 3,500 m) on the premise of deposition relative to the carbonate compensation depth to assure a better comparison with older, predominant shallow water carbonate facies. This follows the notion that biological processes dominate over thermodynamic carbonate transformations at shallower depths (Milliman et al., 1999; Jahnke and Jahnke, 2004; Sarmiento and Gruber, 2004). The abundance of pelagic sediments older than the Cretaceous decreases to almost negligible quantities due to ongoing destruction of oceanic plates at subduction zones preventing the study of pelagic $\delta^{13}C_{carb}$ records in older time intervals. To mitigate inclusion of meteorically altered samples from Permian–Triassic sequences we focused solely on a data-set including boundary profiles situated in Iran (Schobben et al., 2017). These carbonate deposits accumulated on isolated carbonate platforms in the middle of the Tethys ocean (a vast ocean basin that existed throughout the Palaeozoic and early Mesozoic; Muttoni et al., 2009) faraway from continental influences (Ghaderi et al., 2014; Leda et al., 2014). In addition, no obvious signs of exposure to subaerial conditions during the early phases of carbonate rock stabilization, such as palaeokarsts, have been observed in this region (Schobben et al., 2017). The Permian–Triassic boundary is peculiar in that the sedimentation style changed from a skeleton- to microbial-dominated carbonate matrix, a possible consequence of the environmental and ecological destruction associated with the end-Permian mass extinction (Wignall and Twitchett, 1996; Baud et al., 1997). In order to address the potential effect of this carbonate sedimentological turn-over on $\delta^{13}C_{carb}$ variability, the data-set is split in a pre- and post-extinction sample set. The chance that $\delta^{13}C_{carb}$ signatures from decaying terrestrial organics alters the original signal becomes increasingly small for pre-Devonian time intervals—before extensive terrestrial ecosystems developed—although bryophyte, fungal- and prokaryote-dominated terrestrial ecosystems might have existed before that time (Gray, 1985; Horodyski and Knauth, 1994; Wellman et al., 2003; Mills et al., 2018). Moreover, carbonate $\delta^{13}C$ and $\delta^{18}O$ co-variance has been interpreted as evidence for a terrestrial biosphere with a noticeable imprint on the carbonate record back to 850 Ma (Knauth and Kennedy, 2009). To account for this possible meteorically steered C isotope resetting we subdivided the Ediacaran sample set in proximal and distal localities of the Doushantuo and Dengying Formations (see the **Supplementary Information** files for sources). These formations were deposited on the Yangtze Block on top of the cap carbonate of the Cryogenian, with a roughly deepening of sedimentary environments toward the southeast of the terrane

(Zhu et al., 2007). The Precambrian (excluding the Ediacaran) carbon isotope data-set is extracted from the "Precambrian marine carbonate isotope database: Version 1.1" (Shields and Veizer, 2002). Carbon isotope data of this database is filtered and split into two sets. One set contains only samples older than 1,000 Ma, and younger than 1,600 Ma, and thereby represents the Mesoproterozoic; a time period often assumed to be of relative stasis in terms of biotic development (dominated by prokaryotes and to lesser extents eukaryotes) and climatic conditions (Planavsky et al., 2015). The second set contains all other values, and thereby encompasses carbonate rocks deposited during ice-house conditions of the Cryogenian (Sturtian and Marinoan glaciations) (Evans, 2000) and possibly the Palaeoproterozoic (Huronian glaciations) (Evans et al., 1997). This subdivision is useful as it cannot be completely discounted that shallow carbonate deposits, and corresponding carbon isotope imprints, vary in a more systematic manner during icehouse-intervals as opposed to greenhouse worlds, even in the absence of a terrestrial OC flux (Swart, 2008; Bachan et al., 2017). As a result of the scarcity of complete stratigraphic carbon isotope transects, this data-set covers a very broad temporal range as well as lumps data from several stratigraphic units and different geographic regions. This, in contrast, to the Ediacaran and Permian–Triassic data-sets, where data aggregation was limited to single formations and sites from geographically restricted areas. In Sections "Data Processing" and "The Effect of Sedimentation Rate Changes on Carbon Isotope Variability" we will explore whether inclusion of such disparate data-sets with different degrees of sampling resolution, stratigraphic coverage, and sedimentary continuity might bias conclusions drawn from $\Delta^{13}C_{bed-to-bed}$ variation in this data-set.

Data Processing

The philosophy behind the applied data processing protocol is that variation at different stratigraphic resolutions would have been forced by different mechanisms, with high amplitude $\delta^{13}C_{carb}$ variation at the lower-end of stratigraphic resolution tracing microbe-controlled ambient chemical conditions, and differences at the higher-end would be the result of long-term operating of the carbon cycle. Hence, processing of the data-sets follows a simple routine, where first the $\Delta^{13}C_{bed-to-bed}$ variation (following Equation 2) is extracted, whilst adhering to stratigraphic superposition. Subsequently, the obtained $\Delta^{13}C_{bed-to-bed}$ is filtered according to the bed-to-bed distance (or age difference), obtaining three size variation bins; small (distance < 25 cm; or time < 25 ky), intermediate ($25 < d < 100$ cm; or $25 < t < 100$ ky), and large ($d > 100$ cm; or $t > 100$ ky) (**Figure 1**). The oldest three time windows lack precise age models and are reported as the distance between the stratigraphic horizons. In the latter definition, an average time resolution of 1 ky per 1 cm is considered (median net accumulation rates of carbonate deposits from a 10–100 m sequence) (Sadler, 1981), which would be the combined effect of sedimentation rates, sedimentary gaps and compaction after burial, and thereby allowing a rough comparison of bins with either dimensions in distance or time. Usage of time dimensions for the youngest bin is favored, as those sediments had a shorter burial history, and net accumulation might deviate from the older bins. The simplifications adopted here are acceptable since the objectives involve broad over-arching patterns at different ends of the spectrum of $\Delta^{13}C_{bed-to-bed}$ variation through time. Moreover, the conservative low accumulation rate considered here is more likely to dampen the frequency of high amplitude $\Delta^{13}C_{bed-to-bed}$ variation at the small sample spacing bandwidth, than to increase them.

The sampling resolution and total stratigraphic coverage for individual studies varies considerably. This discrepancy may therefore skew the obtained frequency distributions for $\Delta^{13}C_{bed-to-bed}$ variation, where the total $\Delta^{13}C_{bed-to-bed}$ range might be a reflection of the sampling resolution and total stratigraphic coverage. In order to mitigate misrepresentation through the variable sampling resolution and total stratigraphic coverage, we applied a subsampling approach where a sliding window with a bandwidth of 1,000 cm (or 1,000 ky) is routinely applied to obtain a fixed set of the $\Delta^{13}C_{bed-to-bed}$ variation at each of the bandwidths (small, intermediate, and large). The interquartile range (IQR) of $\Delta^{13}C_{bed-to-bed}$ for each subsampling iteration of the stratigraphic sequence is recorded, yielding an average IQR for each time window with a corresponding confidence interval (**Figure 2**).

Numerical Calculations of Whole Ocean Carbon Isotope Changes

In order to evaluate the nature of $\Delta^{13}C_{bed-to-bed}$ variation at different stratigraphic bandwidths, we approximate changes in the DIC-C isotope composition of the whole ocean by numerically solving simple mass-balance calculations in a steady state 1-box model (cf. Kump, 1991; Kump and Arthur, 1999). The steady state assumption is valid for long timescales in respect to the residence time of 100 ky of carbon for the exogenic reservoirs. Noting, however, that the residence time might have been longer during past intervals—a consequence of fundamentally different carbon cycling (Bartley and Kah, 2004; Ridgwell, 2005; Payne et al., 2010). In this model, carbon is transferred from the ocean to the sediments, either as carbonate (F_{carb}) or as organic matter (F_{org}), and enters the ocean through the weathering flux from the continent and mantle-released CO_2 (F_{in}) (**Figure 3**). Changes in the total carbon reservoir (M) can then be written as the expression:

$$\frac{dM}{dt} = F_{in} - \left(F_{carb} + F_{org}\right) \quad (3)$$

The fluxes in- and out of M also have the capability of altering the reservoir's isotope composition (δ_M), where F_{in} is characterized by an isotope value δ_{in} that is usually lower than δ_M and close to the mantle value of $-5‰$ (Derry and France-Lanord, 1996; Kump and Arthur, 1999) (**Figure 3**). The isotope composition of carbonate mineral sedimentation is almost equal to δ_M, as there is no appreciable fractionation during carbonate precipitation (Emrich et al., 1970), albeit that the fractionation slightly deviate for different carbonate minerals and polymorphs (see section "The Impact of Sedimentary Noise on Carbon Isotope Variability"). On the other

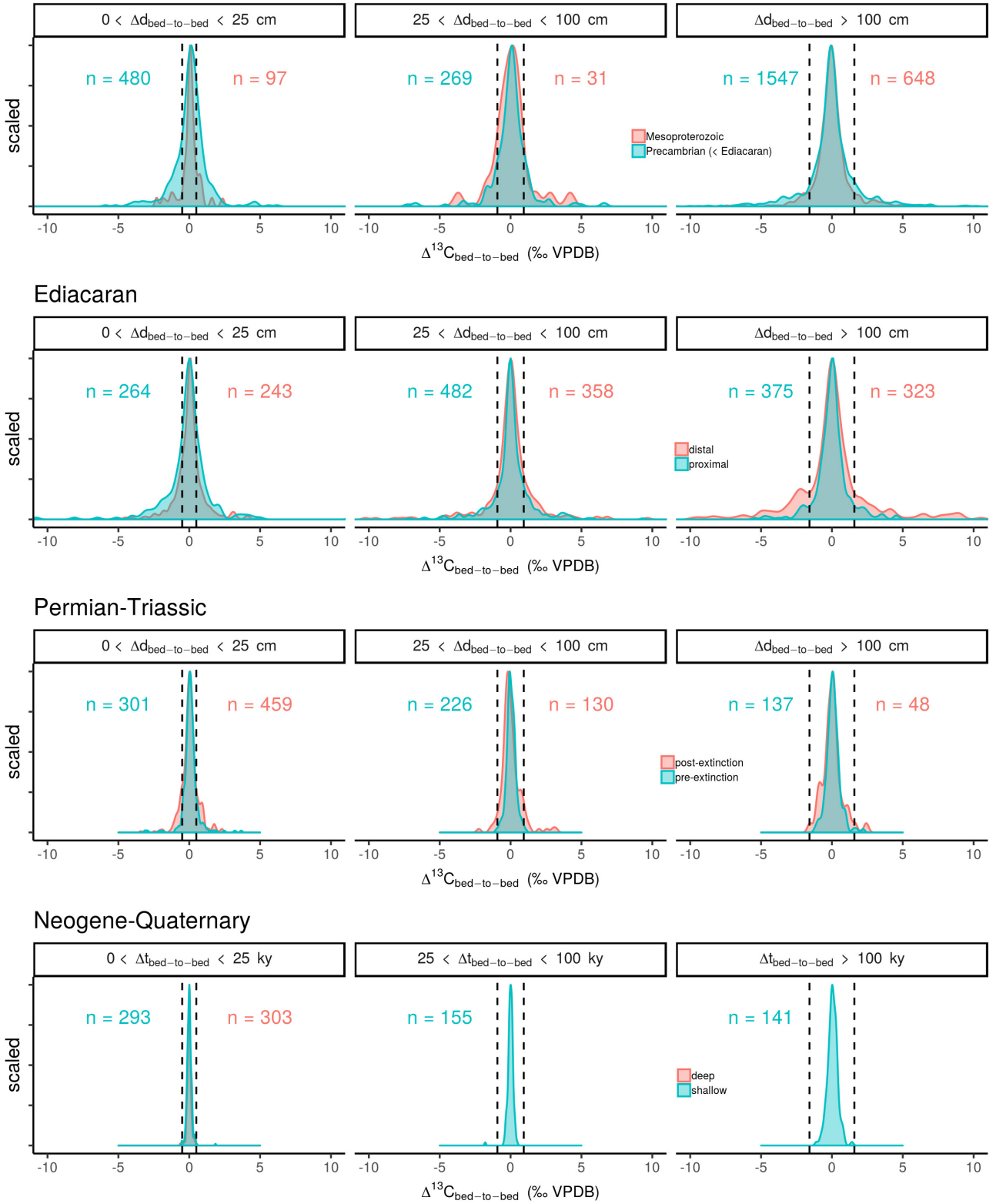

FIGURE 1 | Scaled frequency distributions of $\Delta^{13}C_{bed-to-bed}$, variation for different time intervals and filtered for several bandwidths relating to stratigraphic and temporal resolution of the sampled transects. The dashed line represent the maximum attainable variation in $\delta^{13}C_{carb}$ forced by a two times modulation to lower and higher values for the OC burial flux (*f*), whilst maintaining the other flux and reservoir sizes.

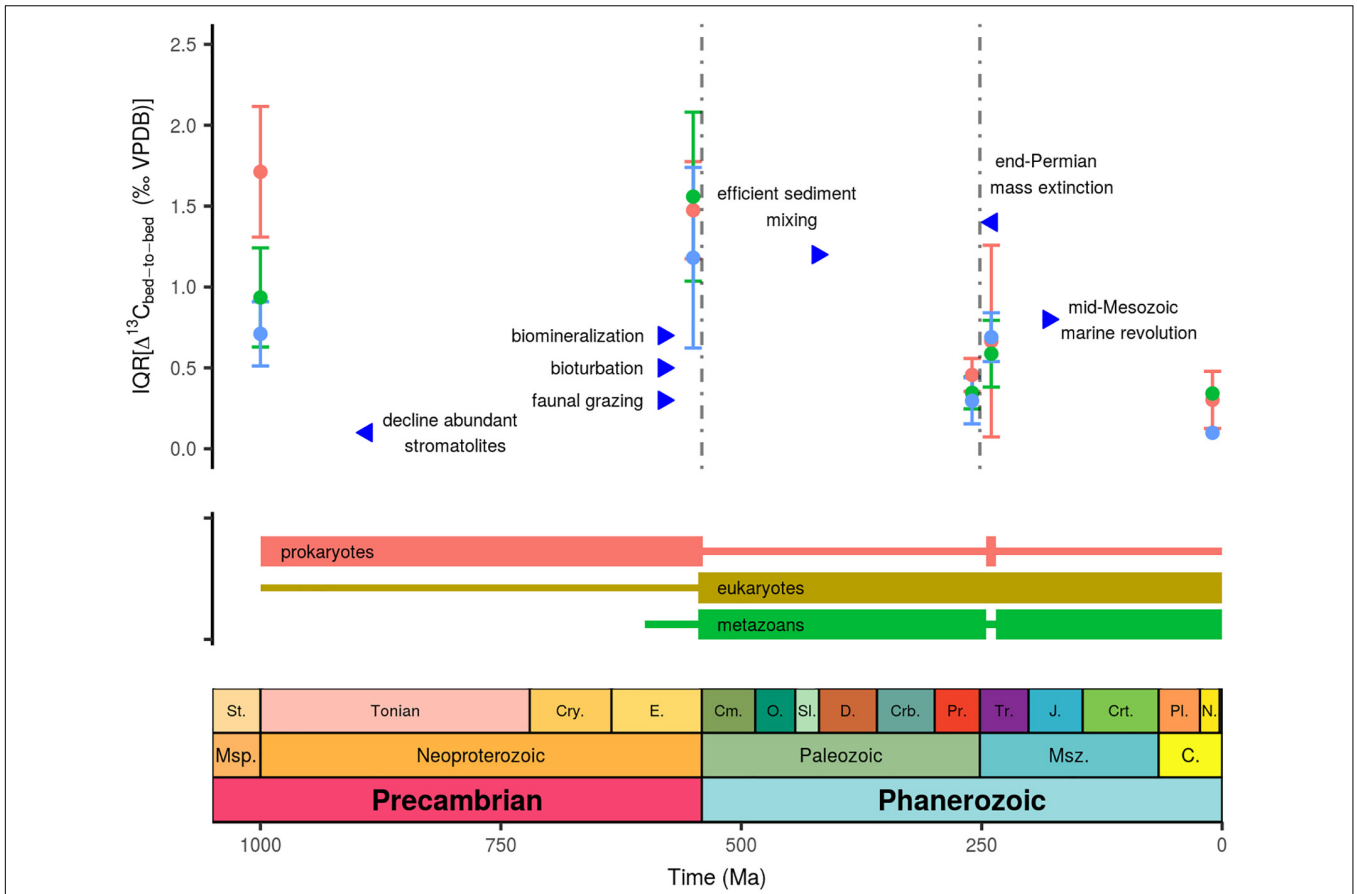

FIGURE 2 | Subsampled $\Delta^{13}C_{bed-to-bed}$ variation expressed as the interquartile range through time, where blue dots denotes the small bandwidth ($d < 25$ cm; or $t < 25$ ky); green demarcates the intermediate bandwidth ($25 < d < 100$ cm; or $25 < t < 100$ ky), and red marks the large bandwidth ($d > 100$ cm; or $t > 100$ ky). See main text for sources of key biological and ecological events.

hand, ^{13}C discrimination (ϵ; expressed in per mil) during organic matter production is large, causing sedimentary organic matter to be on average 30‰ lower than coeval carbonate (Hayes et al., 1999). Although ϵ is assumed constant here, the biologically induced fractionation can vary considerably between organisms and can be affected by environmental factors (Rau et al., 1997; Hayes et al., 1999). The composition of the carbon reservoir then changes according to the following isotope mass balance:

$$\frac{dM\delta_M}{dt} = F_{in}\delta_{in} - \left(F_{carb}\delta_M + F_{org}\left(\delta_M + \epsilon\right)\right) \quad (4)$$

These two equations (3 and 4) can be rewritten by application of the product rule of calculus to explicitly solve for the factors that influence the isotope composition:

$$\frac{d\delta_M}{dt} = \frac{\left(F_{in}\left(\delta_{in} - \delta_M\right) - fF_{out}\epsilon\right)}{M} \quad (5)$$

In equation 5 we assume that OC burial is a fraction of the total flux out of the system ($F_{org} = fF_{out}$). Note also that only the fluxes with an isotope value different than δ_M causes a change in the isotope composition of the reservoir. Reservoir and fluxes sizes as well as their isotopic composition are taken from Arthur (2000). This model configuration was used to gauge the maximum change of δ_M over time periods of 25, 50, and 100 ky (which relate to sample spacing bandwidths: small, intermediate and large of **Figure 1**), by imposing an imbalance to the steady state situation as a 100% increase (and decrease) in f from the starting value of 0.2 (cf. Hayes et al., 1999; Kump and Arthur, 1999). The change in f was initiated at 1 ky, and the change in δ_M at t_x relative to t_0 yields cut-off values, which are depicted as vertical dashed lines in **Figure 1**. Note that the assumptions for bandwidth assignment are based on low median accumulation rates (see section "Data Processing") and that the numerical solutions represent maximum cut-offs for $\Delta^{13}C_{bed-to-bed}$ variation. This approach is thus a conservative approach to approximate the extent of carbon cycle induced modulations of $\delta^{13}C_{carb}$, where actual $\delta^{13}C_{DIC}$ oscillations are likely to have been smaller in amplitude and longer duration (i.e., lower rate of change).

The Effect of Sedimentation Rate Change on Carbon Isotope Variability

In a second exercise we explored the effect of sedimentary gaps within stratigraphic sequences on $\Delta^{13}C_{bed-to-bed}$ variation at different stratigraphic bandwidths. This was done by generating

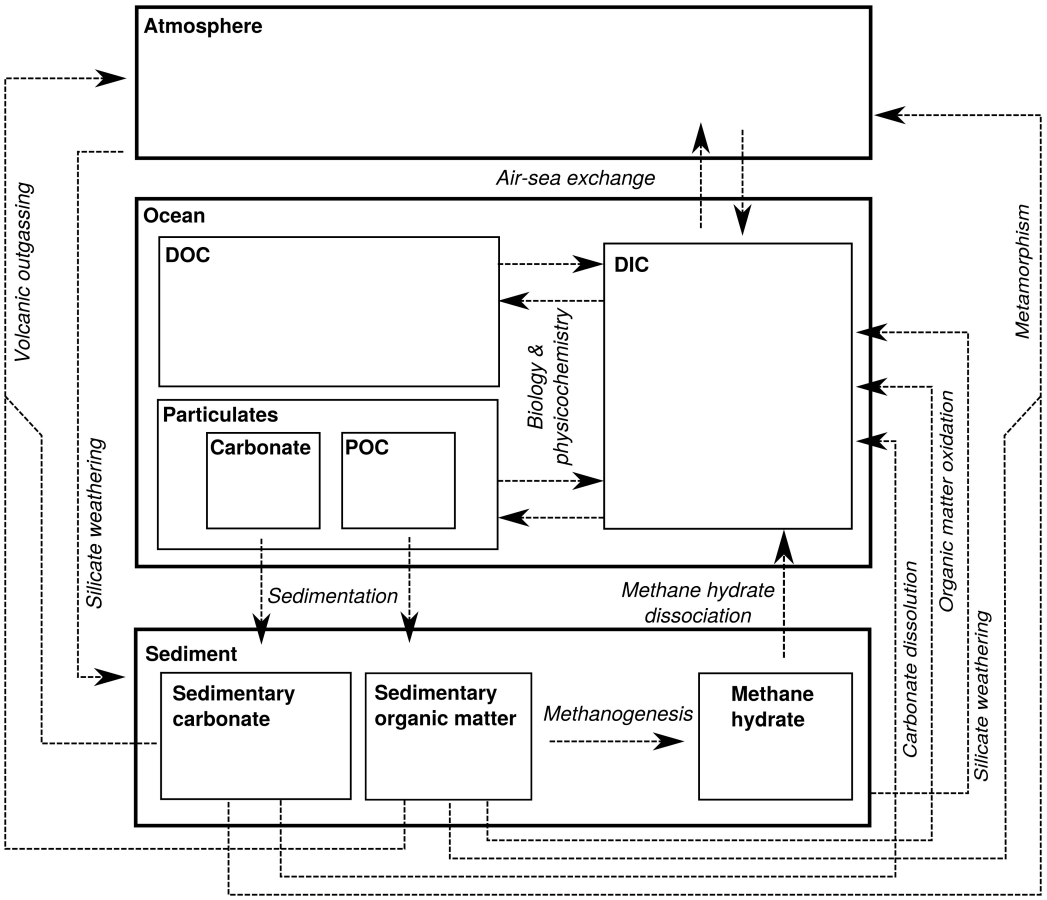

FIGURE 3 | Schematic representation of the biogeochemical carbon cycle with thick-lined boxes representing the major C reservoirs on Earth: the atmosphere, ocean and sedimentary record. The thin-lined boxes represent internal partitioning within these larger C reservoirs. F_{in} is represented by metamorphism, volcanic outgassing and weathering (and episodically methane hydrate dissociation). The flux out of the atmosphere/ocean system is represented by OC burial (F_{org}) and carbonate burial (F_{carb}). Biology and physicochemistry is the sum of carbon fixation, OC remineralization, carbonate precipitation, and carbonate dissolution, which exchanges C between the ocean-internal dissolved inorganic carbon (DIC), dissolved organic carbon (DOC), particulate organic carbon (POC) and carbonate mineral pools.

a virtual 1 My $\delta^{13}C$ time series (**Figure 4A**), which records two simulated perturbations of δ_M by modulating f with a 100% increase relative to the starting value of 0.2, and a subsequent equivalent decrease (relative to the starting value). This time series was, in turn, converted to stratigraphic height (cq. depth) by application of a hypothetical age–depth model (**Figure 4B**). The age–depth model contains variation in sedimentation rate attributed to a virtual sedimentary gap imposed by a third-order sea-level fluctuation (frequency: $\sim 1/10^6$ y), where the initial accumulation of the carbonate platform was set at 2.5 cm ky^{-} (cf. Sadler, 1981), briefly approaching 0 cm ky^{-} at the discontinues surface, and after 200 ky sedimentation commences again at the starting rate (i.e., renewed installment of a carbonate factory). We use median net accumulation rates of carbonate deposits (see section "Data Processing") instead of actual sedimentation rates in this approximation, as it accounts for the reduction in thickness by compaction and small-scaled unconformities (Sadler, 1981). A spline interpolation was used for generation of the curve. Subsequently, interpolations were generated multiple times (n = 100) with slightly varying positions of the hiatus (**Figure 4C**), resulting in a range of age–depth models with cumulative sediment piles that range from 10–30 m (net accumulation rate of 1–3 cm ky^{-}; cf. section "Data Processing"). The age–depth models were then used to convert the virtual 1 My $\delta^{13}C$ time series to dimensions of height. In a final step, the set of $\delta^{13}C_{carb}$ records were subsampled whilst mimicking the random nature of sampling during a field campaign (i.e., varying the sampling resolution throughout the transect). This exercise serves as a null model for $\delta^{13}C_{carb}$ records influenced by sedimentation rate changes, where the frequency distribution of $\Delta^{13}C_{bed-to-bed}$ variation are plotted according to the same protocol as Section "Data Processing" as frequency distributions for the different sample spacing bandwidths (**Figure 4D**).

Computations

The differentials are integrated with the R package *deSolve* (Soetaert et al., 2010) on the open-source platform R (R Core Team, 2018). This document was generated in Rmarkdown

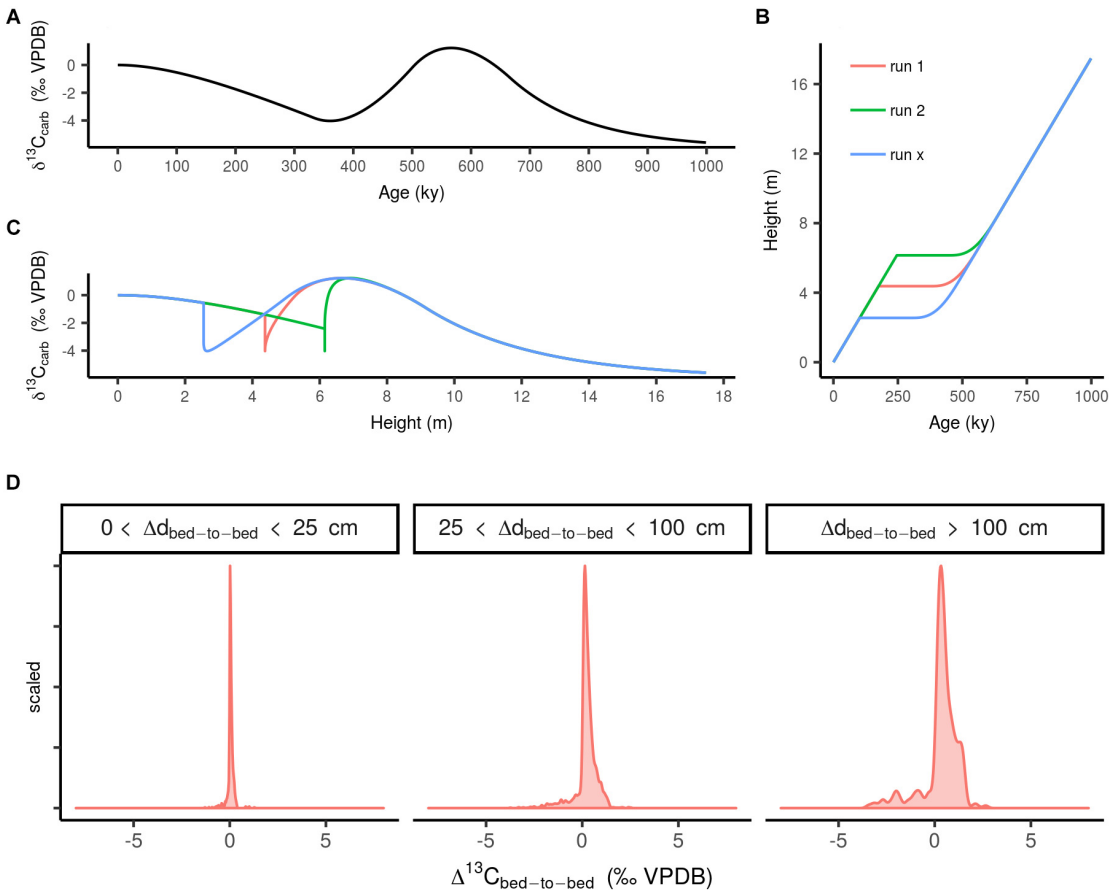

FIGURE 4 | (A) Randomly simulated timeseries of carbon cycle perturbations. **(B)** Age model for the simulated stratigraphic series with a sedimentary hiatus (with runs to exemplify the different simulations, real number of runs is 30). **(C)** The same simulated $\delta^{13}C_{carb}$ sequence but plotted as height and distorted by sedimentary rate changes forced by a third-order sea-level fall and subsequent rise. **(D)** Scaled frequency distribution of $\Delta^{13}C_{bed-to-bed}$ variation for multiple simulations of hiatus-distorted stratigraphic $\delta^{13}C_{carb}$ series.

[*knitr*: Xie, 2014, 2015, 2018, and *kfigr*: Koohafkan (2015)] and data processing and visualization was aided by the R packages: *ggplot2* (Wickham, 2009), *gridExtra* (Auguie, 2017), *gtable* (Wickham, 2016), *stringi* (Gagolewski, 2019), *tidyr* (Wickham and Henry, 2018) and *dplyr* (Wickham et al., 2018). The library *marelac* (Soetaert and Petzoldt, 2018) and the package *seacarb* (Gattuso et al., 2019) were used for marine chemical data and carbonate chemistry calculations, respectively.

RESULTS AND DISCUSSION

Frequency Distributions of Bed-to-Bed Carbon Isotope Variability

The compiled $\Delta^{13}C_{bed-to-bed}$ data (**Figure 1**) show that variation is distributed around a mean (heavy-tailed distribution; see **Supplementary Figure S1**) that is consistently close to zero throughout Earth's history. The same aggregation of data also depicts clear differences in the width of the frequency distribution curves over time, where the oldest two time windows (pre-Ediacaran and Ediacaran) show the broadest spread over all three sample spacing bandwidths (small, intermediate, and large). Proximal sites of the Ediacaran display the largest scatter in $\Delta^{13}C_{bed-to-bed}$ on stratigraphic most-confined scale ($d < 25$ cm), whereas the reverse is observed for $\Delta^{13}C_{bed-to-bed}$ variation at large sample spacing ($d > 100$ cm). By contrast, the intermediate bandwidth produces almost equal-shaped frequency distribution curves for both the distal and proximal sites. The differences between distal and proximal sites of the Ediacaran is, however, small compared to the overall large $\Delta^{13}C_{bed-to-bed}$ spread, suggesting that a potential influx from land-derived organics on bulk rock $\delta^{13}C$ stabilization is of minor importance. A reduction in $\Delta^{13}C_{bed-to-bed}$ variability is observed for the Permian–Triassic at all bandwidths, where a larger $\delta^{13}C_{carb}$ spread can be discerned for the post-extinction microbial dominated world. This pattern hints toward an impact of the extinction event on $\Delta^{13}C_{bed-to-bed}$ variability. The smallest variation in $\Delta^{13}C_{bed-to-bed}$ can be observed in the compilation of ODP core data, where there is no distinction possible in relation to water depth. Note also, that the spread of the data increases with successively larger bandwidths. The same pattern of decreasing stratigraphic-confined carbon isotope

variability with time is produced when applying a subsampling approach (**Figure 2**), excluding the assertion that the sampling strategy dictated the observed signals to a large extent.

Temporal Constraints on Global Carbon Cycle-Induced Carbon Isotope Variations

Bulk rock carbonate carbon isotope records are inferred to track variation in the isotope composition of the ancient DIC pool over time (Scholle and Arthur, 1980; Shackleton and Hall, 1984). By imposing an imbalance in the steady state 1-box model, we can simulate the effect of a carbon cycle reorganization on δ_M (or $\delta^{13}C_{DIC}$) (see section "Numerical Calculations of Whole Ocean Carbon Isotope Changes" and **Figure 3**), and thus put constraints on the maximum $\Delta^{13}C_{bed-to-bed}$ variation per bandwidth. A parameter presumed as a primary driver of $\delta^{13}C_{DIC}$ excursions is the amount of buried organic matter (f), which relates to marine productivity or the OC burial efficiency (Arthur et al., 1988; Kump and Arthur, 1999). With the exception of dramatic events, such as massive volcanism at the Permian–Triassic boundary (Renne et al., 1995) and methane clathrate dissociation at the Palaeocene–Eocene boundary (Dickens et al., 1995), which inject large quantities of ^{13}C-depleted carbon into the exogenic carbon cycle, f can be envisioned to induce recurring $\delta^{13}C_{DIC}$ variation on long timescales (Hayes et al., 1999). In such formulations, it is assumed that weathering, metamorphism and volcanic outgassing remains virtually constant in terms of mass and isotope composition (Shields, 2017). Opposing visions have been proposed, where unroofing and weathering of distinct packages of strata could change δ_{in}, but long-term tectonic driven changes of organic-rich shale versus carbonate weathering are again unlikely and mute variation in δ_{in} (Derry and France-Lanord, 1996). For some of the dramatic Phanerozoic carbon isotope excursions, such as the Mesozoic Ocean Anoxic Events (with durations of >100 ky), f modulations with a ∼50% increase have been proposed (Arthur et al., 1988; Kump and Arthur, 1999). The largest carbon isotope fluctuation of Earth's history; the 'Shuram excursion' (Grotzinger et al., 2011), with $\delta^{13}C_{carb}$ decreasing with ∼12‰ in respect to the background values (and a duration of 25–50 My), has been reconciled with a 60% lowering of f (Shields, 2017). Similarly, Hayes et al. (1999) concluded, based on a paired organic matter–carbonate $\delta^{13}C$ record corrected for variation in ϵ, that f has not likely changed more than a factor of four over the last 800 My (and unfolding over multi-million year timescales). Based on these considerations, we choose a 100% modulation of f (in both the positive and negative direction, with a near-instantaneous perturbation; section "Numerical Calculations of Whole Ocean Carbon Isotope Changes") as an maximum estimated rate of change to gauge whether $\Delta^{13}C_{bed-to-bed}$ variation for each of the bandwidths can conceivably be explained by steady state whole ocean C isotope changes. These cut-off values are depicted as vertical dashed lines in **Figure 1**.

Neogene–Quaternary $\Delta^{13}C_{bed-to-bed}$ variation falls within the calculated maximum attainable whole ocean deviations, based on modulations of f (**Figure 1**). The 'middle Miocene Monterey carbon isotope excursion' is one of the more extreme carbon isotope fluctuation (∼0.5‰ higher $\delta^{13}C_{carb}$) of this time window with superimposed 400ky variation, inferred to relate to a fluctuation in f of ∼25% over a multi-million year interval (Vincent and Berger, 1985; Corfield and Cartlidge, 1993; Derry and France-Lanord, 1996; Holbourn et al., 2007). The systematics of this time window therefore suggest that carbonate rock $\delta^{13}C$ follows seawater $\delta^{13}C_{DIC}$, and that $\Delta^{13}C_{bed-to-bed}$ deviation is likely caused by reorganizations of the global-scale biogeochemical carbon cycle. This proof of concept supports extrapolation of this approach further back in time.

The most notable result for the older time windows is that all of them contain $\Delta^{13}C_{bed-to-bed}$ variation that are not readily explained by steady state evolution of the carbon reservoirs (**Figure 1**). This is especially true for all of the bandwidths with a narrow sample spacing (d < 100 cm). Alternative scenarios relating to non-steady state dynamics, intrinsic variation of sedimentation and the sedimentary archive, the multi-component nature of bulk rock, and ambient chemical conditions during lithification, must be invoked to explain these deviations in $\Delta^{13}C_{bed-to-bed}$ (see below). Moreover, considering the prevalent high atmospheric CO_2 state—and thus large oceanic DIC reservoir—during most of the older studied time intervals suggest that the resistance of the system to change must have been even higher (Kump and Arthur, 1999; Arp et al., 2001; Bartley and Kah, 2004; Payne et al., 2010). Adopting a marine carbon reservoir size from the Quaternary ice house state for the calculated cut-off values can therefore be used a conservative measure to gauge the nature of $\Delta^{13}C_{bed-to-bed}$ variation. Thus an even larger fraction of the variation might not follow $\delta^{13}C$ systematics as dictated by the global C cycle. However, flux sizes could also have waxed and waned in conjunction with the DIC reservoir size through time and/or some carbon sinks (e.g., authigenic carbonate) might have been overlooked, dampening again the resistance of marine DIC to C isotopic perturbations (Schrag et al., 2013; Shields, 2017), justifying our conservative approach.

Non-steady State Dynamics and Carbon Isotope Variations

An often cited mechanism for extreme negative deviations in $\delta^{13}C_{carb}$ as observed in the Neoproterozoic (e.g., the Ediacaran Shuram excursion; **Figure 2**) is a non-steady state mechanism, whereby a large recalcitrant dissolved organic carbon (DOC) reservoir is partly oxidized. In this model formulated by Rothman et al. (2003), the ocean DOC reservoir of the Neoproterozoic is assumed unusually large compared to modern levels (100 times larger). When invoking this scenario to explain the Ediacaran Shuram excursion (with a duration of 25–50 My), the oxidant demand posed by the oxidation of such a large DOC pool would strip the atmosphere's O_2 at present levels within 800 ky (Bristow and Kennedy, 2008). Although it seems difficult to reconcile this model with the duration of long-term $\delta^{13}C_{carb}$ trends (i.e., the Shuram excursion), it could be compatible with deviation in $\Delta^{13}C_{bed-to-bed}$ at small stratigraphic scales throughout the Ediacaran Doushantuo and Dengying Formations (i.e., the

Ediacaran data-set). One critical point in this scenario is, however, the difficulty of spatially separating the pools of reduced C (DOC) and oxidants. A state; which should then be episodically perturbed to cause mass oxidation of the DOC pool in order to introduce ^{13}C-depleted C to the DIC pool. Even though ocean mixing might have been sluggish during some intervals, physical constraints put an upper limit of several thousand years on the ocean mixing time, which is maintained either through seawater cooling and sea-ice brine expulsion at high latitudes or elevated evaporation and increased salinity at subtropical latitudes (Hotinski et al., 2001; Zhang et al., 2001). The haline mode of circulation is more sluggish but also highly unstable (Zhang et al., 2001). A possible scenario would entail that the DOC pool grows in a sluggish ocean, whilst episodic thermal-controlled ocean mixing ventilates the ocean, causing transient events of DOC oxidation. These transient events could haven transferred to the carbonate archive as a more variable carbon isotope signal (i.e., increased occurrence of higher amplitude $\Delta^{13}C_{bed-to-bed}$). Unfortunately, a lack of high-resolution climate records for these ancient time intervals makes it impossible to test such scenarios. Climate data is limited to broad temporal patterns which suggest phases of low- and mid-latitude glaciation during the Cryogenian (Sturtian and Marinoan glaciations) (Evans, 2000) and possibly the Palaeoproterozoic (Huronian glaciations) (Evans et al., 1997). Note, that the difference between the two subsets with- and without icehouse intervals of the pre-Ediacaran data-set is only marginal (**Figure 1**), and might even suggest larger $\Delta^{13}C_{bed-to-bed}$ at intermediate stratigraphic scales for the latter subset. Evidence for cold climatic stages and possible transitions to more invigorated ocean turnover in the Mesoproterozoic, Ediacaran and Permian–Triassic are ambiguous, and are generally viewed as warm intervals (Wignall and Twitchett, 1996; Evans, 2000; Planavsky et al., 2015). So, while a possible DOC-driven broadening of the $\Delta^{13}C_{bed-to-bed}$ spectrum cannot be completely ruled out, it is unlikely within the current state of knowledge.

Catastrophic ^{13}C-depleted carbon release (on intervals shorter than the residence time of carbon in the ocean/atmosphere system) has been forwarded to explain negative excursions in the Phanerozoic $\delta^{13}C_{carb}$ record. For example, negative $\delta^{13}C_{carb}$ excursions recorded in carbonate and organic compounds of the Palaeocene–Eocene boundary and Triassic–Jurassic boundary have been connected with the dissociation of methane hydrate deposits (Dickens et al., 1995; Ruhl et al., 2011). Introduction of methane to the global carbon reservoir with a $\delta^{13}C$ of −60‰ is sufficient to perturb global $\delta^{13}C_{DIC}$ with several per mil, whilst only mobilizing a fraction of the global methane hydrate reservoir. Although these events would be dramatic and short-lived, compatible with at least some of the spread in $\Delta^{13}C_{bed-to-bed}$ variation, the regeneration of the methane hydrate reservoir will not exceed the OC burial flux (**Figure 3**) (Kvenvolden, 2002). Hence, recurring events of methane hydrate dissociation are difficult to reconcile with the frequency of high amplitude $\Delta^{13}C_{bed-to-bed}$ variation in especially the shorter time windows (<1.5 My duration of the Permian–Triassic window: **Figure 1**).

There are several other processes that act on timescales much shorter than the residence time of carbon in the exogenic reservoirs, and closer to the ocean mixing time (<1 ky). For example, changes in pH and alkalinity affect $\delta^{13}C_{DIC}$ through the specific equilibrium fractionation associated with the different dissolved inorganic carbon species (Zhang et al., 1995). Transient oceanic pH changes have potentially occurred in the geological past, and are related to rare catastrophic CO_2 injections (Hönisch et al., 2012). The rarity of these events combined with the limited impact of a CO_2 rise on the well-buffered ocean, of conceivably not more than one unit on the pH-scale (Caldeira and Wickett, 2003; Tyrrell and Zeebe, 2004; Hönisch et al., 2012), and less than one per mil deviations in $\delta^{13}C_{DIC}$ (**Figure 5**; Zhang et al., 1995), can only explain a minor portion of the $\Delta^{13}C_{bed-to-bed}$ variation at any given interval. The same empirically derived function for the equilibrium fractionation between DIC and CO_2 in the air (ϵ_{DIC-g}) does, however, show a strong dependence on temperature (**Figure 5**; Zhang et al., 1995). If indeed this temperature relationship can alter the C isotopic composition of oceanic DIC, it could potentially explain some of the $\Delta^{13}C_{bed-to-bed}$ variance, when one envisions dramatic fluctuations in sea-water temperature on short timescales. The latter is difficult to evaluate as this temperature dependence of $\delta^{13}C_{DIC}$ is again a function of atmosphere–ocean equilibration and ocean circulation, which, in turn, abides to temperature and pCO_2 (Galbraith et al., 2015).

Alternatively, surface water primary productivity is known to create a depth gradient of $\delta^{13}C_{DIC}$, where C fixation by photosynthetic organisms causes successive ^{13}C-enrichment of the remaining DIC, and settling organic particles at depth

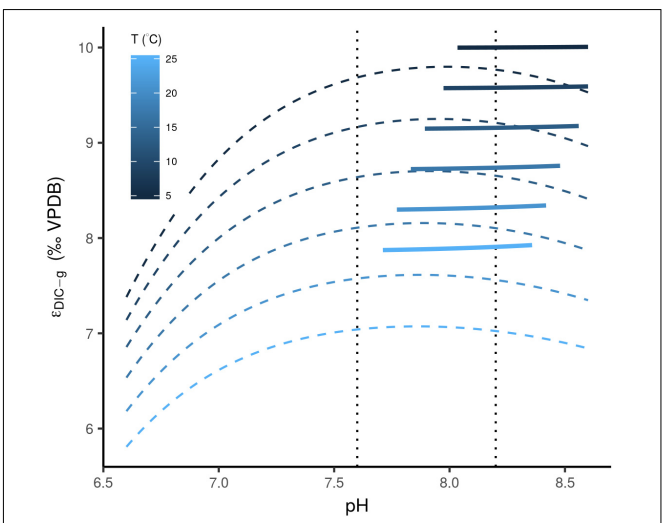

FIGURE 5 | Calculated equilibrium fractionation, after Zhang et al. (1995), between DIC and CO_2 in the air (thin dashed lines), based on the concentrations of aqueous carbon species, and ϵ_{DIC-g}, based on an empirically derived relationship (thick lines). Values are plotted over pH and temperature ranges representative for aquatic environments. Note, that the empirically obtained ϵ_{DIC-g} are only plotted for fCO_3^{2-} values in the range of 0.05 and 0.2. The vertical stippled lines depict the predicted range of pH change over the last 100 My (Tyrrell and Zeebe, 2004).

remineralize, causing the bottom water DIC pool to be depleted in ^{13}C. This biological pump, in conjunction with ocean circulation and atmosphere–ocean exchange of C, maintains a dynamic equilibrium between $\delta^{13}C_{DIC}$ of deep- and surface water (Hsü and McKenzie, 1985; Rampino and Caldeira, 2005; Galbraith et al., 2015). Changes in primary productivity, ocean circulation, and atmosphere–sea exchange of CO_2 can therefore alter the difference between $\delta^{13}C_{DIC}$ of the surface water and bottom water. The aforementioned example of a dynamic equilibrium operates on a restricted spatial scale, and therefore can conform to geographically distinct $\delta^{13}C_{DIC}$ of the water column. Spatially differential $\delta^{13}C_{DIC}$ and carbonate mineral deposits are, for instance, known from distinct water masses and basins. For example, Holbourn et al. (2007) showed in a compilation of the middle Miocene that $\delta^{13}C_{carb}$ of the South Pacific is 0.5‰ higher than coeval values of the northwestern sector of the Pacific. The most famous case of a wholesale productivity collapse, e.g., as advocated for the aftermath of the mass extinction at the Cretaceous–Palaeogene boundary, is also known as a "Strangelove ocean," and had been connected with a distinct C isotope imprint in the sediment record (Hsü and McKenzie, 1985). This scenario has been largely discounted subsequently as a certain degree of OC transport to the ocean floor must have persisted to prevent the ocean DIC-C isotope composition to have plummeted to values equal to the riverine (δ_{in}) value (Kump, 1991 and section "Numerical Calculations of Whole Ocean Carbon Isotope Changes"). However, scenarios of a reduced OC sinking flux and increased atmosphere–sea exchange of carbon under greenhouse conditions might have induced a dampening of the 1–2‰ $\delta^{13}C_{DIC}$ depth gradient (D'Hondt et al., 1998; Galbraith et al., 2015). Again, the most extreme cases with several per mil change only occur over long time-intervals (Kump, 1991) and are therefore incompatible with large amplitude $\Delta^{13}C_{bed-to-bed}$ variation at the lower-ends of stratigraphic resolution.

The Impact of Sedimentary Noise on Carbon Isotope Variability

Carbonate carbon isotope variation can as well be an expression of factors intrinsic to the mineral assemblage, sedimentary environment and subsequent lithification of the sediment pile. For example, the carbonate archive consists of a wide spectrum of carbonate minerals and polymorphs (e.g., calcite and aragonite) which all adhere to a specific thermodynamically controlled C isotope fractionation during formation under equilibrium (Rubinson and Clayton, 1969; Grossman, 1984a; Romanek et al., 1992; Jimenez-Lopez and Romanek, 2004). Hence variation in the predominant carbonate minerals and polymorphs accumulating through time, as a consequence of a changing depositional setting or large-scale ocean chemistry, changes could therefore explain part of the here identified $\Delta^{13}C_{bed-to-bed}$ variation (e.g., Swart, 2008). However, these equilibrium isotope fractionations can only account for ∼1 per mil of variation, if one would consider a 100% change in mineralogy from bed-to-bed.

A second source of intrinsic $\delta^{13}C$ variation of the carbonate archive links to the summed effect of primary and authigenic metastable carbonate mineral stabilization by dissolution–recrystallization in the early diagenetic domain, and is a principal aspect of this study. The alteration of the carbonate record does, however, not stop after early diagenetic stabilization, and with successive burial the sediment pile can be subjected to increasing pressure and temperature (e.g., Urey, 1947). A recent study by Bernard et al. (2017) has reinvigorated the debate on the effect of burial diagenesis and solid-state diffusion on the $\delta^{18}O$ composition of calcareous skeletons. In this experiment foraminifera test subjected to high temperatures in an attempt to simulate the burial environment were shown to re-equilibrate to varying degrees at fine spatial scales with the surrounding fluid. Albeit an important observation, the effect is likely of less importance for inducing small-scale variation in C isotope composition of carbonate, based on several observations: (1) diminishing reactivity of coarsened carbonate crystals during early diagenetic recrystallization might effectively shield the minerals for further alteration during deeper burial (Banner and Hanson, 1990), (2) the temperature dependence of equilibrium C isotope fractionation during carbonate precipitation is small (Emrich et al., 1970), and (3) as opposed to the early diagenetic environment with relatively labile OC sources and strong gradients in solutes, the deep burial environment lacks large and spatially variable allochthonous carbon sources (Banner and Hanson, 1990).

Lastly, the fundamentally incomplete geological record, with gaps ranging from grain boundaries to unconformities (Barrell, 1917; Sadler, 1981; Dott, 1983), raises the question whether the $\Delta^{13}C_{bed-to-bed}$ variation might be an artifact of the lack of stratigraphic completeness. A predominant factor in stratigraphic completeness of carbonate deposits is water depth and the accommodation space of the sedimentary basin, which is influenced by sea-level change and tectonics. The waxing and waning (i.e., the frequency) of sea-level occurs at timescales ranging from multi-million to thousands of years and from high-amplitude change (up to 200 m), by the growth and decay of continental ice sheet, to low-amplitude, by continental groundwater storage/discharge and thermal expansion/contraction of seawater (Jacobs and Sahagian, 1993; Miller et al., 2005).

Considering this notion of completeness, we set-up an experiment to deduce the effect of a third-order sea-level fluctuation (frequency: $\sim 1/10^6$ y) on $\Delta^{13}C_{bed-to-bed}$ variation (see section "The Effect of Sedimentation Rate Changes on Carbon Isotope Variability" and **Figure 4**). In this scenario it is assumed that a third-order sea-level cycle has a high probability of interrupting the average sampled sequence [i.e., which consists of one or two formations with a (multi-)million year duration]. The results of this exercise ('a null model': **Figure 4D**) shows that $\Delta^{13}C_{bed-to-bed}$ variation at small stratigraphic scales are likely not amplified by a lack of stratigraphic completeness. This null model serves best to approximate the effect of lumping $\Delta^{13}C_{bed-to-bed}$ from records that do not always overlap in time, such as for the pre-Ediacaran time window. Admittedly there are many more processes at multiple temporal scales that can disturb sedimentary continuity (e.g., reworking and

dissolution) then the here postulated influence of third-order sea-level changes. As a general rule, stratigraphic completeness of a section becomes more compromised when smaller time scales are subject of investigation (Sadler, 1981), as such increased noise in $\Delta^{13}C_{bed-to-bed}$ could be an apparent signal caused by this effect. Nevertheless when comparing $\Delta^{13}C_{bed-to-bed}$ from all time windows (**Figure 1**), we see an increased or comparable amount of variation with increasing bandwidth. This pattern cannot be reconciled with this inverse relation of stratigraphic resolution and completeness. Clearly more rigorous tests are required in the future, which introduce different aspects of the noisy sedimentary record. Nonetheless, we conclude that this exercise serves as a useful first attempt to assess the potential influence of stratigraphic completeness on $\Delta^{13}C_{bed-to-bed}$.

Carbon Isotope Variability and the Evolution of the Biosphere

Our deductive assessment of potential drivers behind stratigraphic-confined carbon isotope fluctuations stipulates the need for involving the nature of the isotope recorder—the diagenetically stabilized end-member of a multi-component carbonate mineral assembly. A subset of large amplitude $\Delta^{13}C_{bed-to-bed}$ variation in the older time intervals are not readily corroborated with the presumed default functioning of the global carbon cycle, rare non-steady state dynamics, mineralogy and the incompleteness of sedimentary records. Large amplitude carbon isotope fractionation, however, is an integral aspect of enzymatic reactions (i.e., kinetic reactions), and the products of these enzymatic reactions are isotopically distinct from the global marine $\delta^{13}C_{DIC}$ signature (e.g., Rau et al., 1997; Hayes et al., 1999). Besides this dichotomy in $\delta^{13}C$ composition of organic and inorganic carbon, several other prerequisite are needed to funnel such metabolic C isotope signatures directly into the carbonate archive (as opposed to long-term evolution of marine $\delta^{13}C_{DIC}$ driven by the carbon cycle). One such aspect is the creation of micro-environments; e.g., a cell-membrane can create a solute that is distinct from its ambient surrounding. Together enzymatic reactions and compartmentalization (membrane enclosed regions), can create physiologically controlled gradients which can be amplified by reduced effective diffusion rates and high metabolic rates, such as occurring in microbial mats. Microbial mats consist of microbial communities which secrete gel-like exopolymeric matrices, or biofilms, which are signified by steep gradients in, e.g., oxygen, sulfide, and light, but also in, for instance, ^{13}C isotope (Arp et al., 1999, 2001; Visscher and Stolz, 2005; Andres et al., 2006). Furthermore, metabolic carbon isotope signatures imprinted on DIC have been shown to arise from restricted water mass exchange in terrestrial aquatic systems (Bade et al., 2004). As an analog, the diagenetic environment with restricted water mass replenishment, and ongoing decay of organic matter with depth, can act as a conduit which creates metabolic $\delta^{13}C_{DIC}$ signatures that can end-up in diagenetic carbonate precipitates via dissolution–recrystallization reactions (Irwin et al., 1977; Schobben et al., 2017). Hence these notions are a viable alternative to induce spatially and temporally restricted C isotope scatter, which outweighs other mechanisms in their maximum attainable amplitude (Schobben et al., 2017). Moreover, such metabolic C isotope signatures have already been proven to be of significance for modern and ancient bulk rock and bio-mediated carbonate deposits (Andres et al., 2006; Birgel et al., 2015; Cui et al., 2017). The question, however, remains to what extent these signals have persisted and evolved over Earth's history in conjunction with the evolution of life (**Figure 2**).

Microbial mat communities exhibit spatial and temporal heterogeneity of the microbial populations, arranged based on their metabolism (e.g., photoautotrophs, aerobic, and anaerobic heterotrophs and chemolithotrophs) (Visscher and Stolz, 2005), thereby potentially serving as a catalyst for a highly diverse palette of $\delta^{13}C$ signatures. Furthermore, the same microbial mat communities can induce carbonate precipitation (Arp et al., 2001; Dupraz and Visscher, 2005; Visscher and Stolz, 2005), thereby providing a means of capturing these diverse $\delta^{13}C$ signals. Hence $\Delta^{13}C_{bed-to-bed}$ variation can be envisioned to be an emergent property which emanates from this micro-scale heterogeneity, where local physical and biological aspects steer the isotope variation in microbial mat communities. The demise of abundant stromatolites already before the Ediacaran (Awramik, 1971; Walter and Heys, 1985) might seem contradictory to the notion of heterogeneous microbial mat communities and associated C isotopic variation, as the amplitude of stratigraphic-confined $\Delta^{13}C_{bed-to-bed}$ variation increases during the Ediacaran (**Figure 2**). The advent of faunal grazing has been linked to decline of abundant stromatolites, as stromatolites nowadays occur in harsh environments (hypersaline and high temperature) where grazers are excluded (Walter and Heys, 1985). Note, however, that microbial carbonate build-ups do not completely disappear but seem to change in fabric to predominantly clotted forms without internal lamination (thrombolites; Arp et al., 2001). It has therefore been proposed that this turn-over reflects a change in the ocean's carbonate chemistry; notably increasing Ca^{2+} concentrations (Arp et al., 2001). As an alternative viewpoint, the rapid development of the biosphere in the Ediacaran (Butterfield, 2007) and a more effective biological pump, aided by fecal pellet production and an overall size increase of organisms (Logan et al., 1995; Butterfield, 2009, 2018; Payne et al., 2009; Meyer et al., 2016), might all have increased spatial and temporal $\delta^{13}C_{carb}$ heterogeneity. In this scenario $\Delta^{13}C_{bed-to-bed}$ variability relates to the early diagenetic environment, where the patchy distribution of accumulated organic matter and (sub-)seafloor microbial communities control the C isotope trajectory imprinted on pore-occluding cements and recrystallized precipitates. Indeed Cui et al. (2017) uncovered ^{13}C-depleted diagenetic cements in bulk rock from the Ediacaran Doushantuo Formation (South China), which these authors related to episodic enhanced anaerobic oxidation of methane by microbes.

On the opposite end, there is also the need to explain why these metabolic $\delta^{13}C$ signatures, in turn, diminish over the Phanerozoic, and are completely absent in the later

parts of the Cenozoic. Differently phrased: what erased this variability from the $\delta^{13}C$ record? Certain key biological and ecological innovations occurred across Earth's history, which have been inferred to have drastically impacted the chemistry of the ocean and the sedimentary archive (Knoll, 2003; Zeebe and Westbroek, 2003; Hazen et al., 2008; Meyer et al., 2016). Notably the transition into the Phanerozoic saw the radiation of metazoans and the gradual infaunalization of benthic organisms, which began to steer and irrigate sediments more effectively (Canfield and Farquhar, 2009; Tarhan et al., 2015). Combined these aspects are known as bioturbation and refer to the displacement of particles by animals (sediment mixing) and flushing of burrows for respiratory and feeding functions (bio-irrigation) (Kristensen et al., 2012). Both factors dampen spatial variability of organic matter in sediments through dispersion and more-effective remineralization of organic matter in the surface layers. Enhanced dispersion of OC can then lower the spatial and temporal variability of the $\delta^{13}C$ record that would be incorporated in diagenetic precipitates (Schobben et al., 2017). Extensive reworking of the sediment by biota only occurred later in the Palaeozoic (Tarhan et al., 2015), an observation compatible with enlarged $\Delta^{13}C_{bed-tob-bed}$ variation in the Ediacaran and subsiding scatter in the later Phanerozoic $\delta^{13}C_{carb}$ record (**Figure 2**).

The advent of obligate enzymatic skeletonization from the Late Ediacaran onward would have successively added calcareous skeletons to the sediment. These skeletons would have mainly formed above the sediment–water interface with a virtually unrestricted pool of DIC and thus with limited $\delta^{13}C_{carb}$ variability. Note, however, that infaunal calcifiers do contribute to the sediment record as well, and skew this inference by incorporating porewater $\delta^{13}C_{DIC}$ that may poorly reflect contemporaneous oceanic values (Grossman, 1984a,b; Fontanier et al., 2006, 2008). And, although, often assumed to be precipitated in close equilibrium with marine DIC, yielding particularly smooth $\delta^{13}C_{carb}$ stacks (e.g., Zachos et al., 2001), heterogeneity in $\delta^{13}C_{carb}$ at small spatial scales have been found in calcite and aragonite produced by deep-water corals, brachiopods and foraminifera (Spero and Williams, 1988; Adkins et al., 2003; Auclair et al., 2003; Blamart et al., 2005). This variation is thought to be induced by; pH variation in the intracellular calcification fluid, growth rates, ontogonetic stages, respiratory CO_2 and symbionts, and are collectively known as 'vital effects.' The cumulative scattering of these micro-habitat and vital effects imposed on $\Delta^{13}C_{bed-tob-bed}$ from carbonate predominated by enzymatic skeletonization is hard to judge at this stage, but seems to be of marginal importance in the current compilation (**Figure 1**).

The decline $\Delta^{13}C_{bed-tob-bed}$ variation in the Palaeozoic might therefore relate to more extensive bioturbation, faunal grazing, and possibly larger contributions from calcareous skeletons, or a combination of all those factors. The importance of these factors is further enforced by comparing the pre- and post-extinction record of the end-Permian mass extinction, where there is a return of higher amplitude $\Delta^{13}C_{bed-to-bed}$ (**Figure 2**). This extinction event marks the most drastic post-Cambrian biodiversity decline and has been linked to reduced sediment mixing (Wignall and Twitchett, 1996) and a turnover from skeleton- to microbial-dominated carbonate deposits (Baud et al., 1997). These turnovers have been reconciled with higher internal C isotope variability of post-extinction carbonate rock, yielding a noisier $\delta^{13}C_{carb}$ record (Schobben et al., 2017).

The sustained drop in the amplitude of $\delta^{13}C_{carb}$ variation when moving to the Cenozoic can be attributed to significant biological events in the Mesozoic (**Figure 2**). Firstly, bio-mediated precipitates decline from the Triassic onward (Webb, 1996). Secondly, this change has been connected to biological radiation of pelagic calcifiers (planktonic foraminifera and coccolithophorids) that exerted a primary control on the carbonate chemistry, inducing a lowering of DIC and Ca^{2+} concentrations (Arp et al., 2001; Zeebe and Westbroek, 2003; Ridgwell, 2005). Besides reducing the potential for bio-mediated carbonate precipitates to develop under less-carbonate saturated conditions, this turnover spawned another increase in calcareous skeleton production. As exemplified by the above example, these biological and ecological innovations could have been intrinsically linked, and it is therefore tempting to encapsulate the change in the $\Delta^{13}C_{bed-to-bed}$ amplitude to a developing biosphere. Considering the long delay in the development of more "complex" life on Earth (for reasons not yet fully understood), this state of highly variable $\delta^{13}C$ of the carbonate archive might have persisted over a long time interval. Future studies could focus on better refining the temporal and spatial trends in $\Delta^{13}C_{bed-to-bed}$ variation, by high-resolution (cm-scale) sampling of Precambrian rock sequences, which is only marginally represented in the currently used database, and by comparative studies of coeval bioturbated and un-bioturbated strata in Phanerozoic strata or modern environments. If indeed these large-scale patterns of spatially and temporally confined carbon isotope variability reflect on underlying biological processes, they may also serve as a baseline to establish the biogenicity of carbonate deposits. The search for life on other planets could potentially be aided by looking for such emergent properties of microbial life. The latter is furthermore advantageous, as the C cycle on extraterrestrial worlds might be different, but metabolic steered isotope fractionations and concomitant spatially restricted $\delta^{13}C$ variability might be a more universal aspect of carbonate deposits in a prokaryote-dominated world.

CONCLUSION

Broad-scale stratigraphic trajectories of changes in the C isotope composition of the marine carbonate archive are a focal point for palaeontological, palaeo-environmental and stratigraphic studies. Much less emphasis is placed on stratigraphic-confined $\delta^{13}C_{carb}$ fluctuations (bed-to-bed), which are often discarded as mere outliers and noise. By analyzing a comprehensive C isotope data-set capturing discrete time windows of the last ~2.5 billion year, and highlighting the multi-component nature of bulk carbonate samples, we show that stratigraphic-confined $\delta^{13}C_{carb}$

fluctuations are most convincingly explained by microbial metabolic activity captured in authigenic and diagenetic mineral additions. Stratigraphic-confined C isotope variation was measured as bed-to-bed C isotope differences at varying bandwidths (ranging from less than 25 cm to more than 100 cm). A subset of pre-Cenozoic $\Delta^{13}C_{bed-to-bed}$ variation is not easily reconciled with normal operating of the global-scale biogeochemical carbon cycle, based on steady-state box model calculations. Furthermore, the amplitude of the obtained $\Delta^{13}C_{bed-to-bed}$ variation exhibit a decreasing trend over Earth history, which are highest during the Precambrian and start to fall over the Phanerozoic. An exception to this trend is the return of $\Delta^{13}C_{bed-to-bed}$ in the extinction aftermath of the end-Permian biotic crisis, which eliminated many metazoan taxa. No other convincing mechanism (i.e., non-steady state behavior of the C cycle and stratigraphic incompleteness) then the smoothing effect of a developing biosphere can give a satisfactory explanation for the aforementioned features of the long-term $\Delta^{13}C_{bed-to-bed}$ record. In this scenario it is envisioned that a prokaryote-dominated biosphere is linked to heightened spatial diversity in authigenic and diagenetic C isotope signal incorporation, fueled by a diverse set of metabolic pathways in conjunction with compartmentalization (membrane enclosed regions), elevated metabolic rates and reduced diffusion rates in biofilms, as well as restricted water mass exchange in a heterogeneous diagenetic environment. The eradication of these (sub-)seafloor micro-environments was initiated with the development of a metazoan-dominated biosphere (in the post-Ediacaran) that actively stir sediments, graze upon the substrate, but potentially also the advent of obligate calcification (e.g., corals, mollusks, foraminifera, and coccolithophorids). Although this scenario is an initial assessment of the $\Delta^{13}C_{bed-to-bed}$ variation, and it is not possible to delineate with certainty which biological and ecological trades cause (or erase) $\Delta^{13}C_{bed-to-bed}$ variation, it highlights the need for alternative approaches to extract palaeontological and palaeo-environmental information from the carbonate archive. Such advancements might also be useful in the search for life on other planets, as isotope fractionations during metabolic reactions are likely a universal aspect of life. Hence variability in the isotope chemistry at confined spatial scales of carbonate rock might be a more widely applicable signature for life.

CODE AVAILABILITY

The code used for data processing, statistics and numerical modeling is written in the R language and is included in the **Supplementary Files**.

AUTHOR CONTRIBUTIONS

MS conceived and designed the study. MS and BvdS contributed intellectual input and wrote the manuscript.

ACKNOWLEDGMENTS

We are grateful for discussions with Graham Shields (University College London) and constructive comments by the three reviewers on earlier work that significantly improved the manuscript. The NWO (NWO ALW 0.145) and the Utrecht University Library Open Access Fund are acknowledged for funding.

SUPPLEMENTARY MATERIAL

The Supplementary Material for this article can be found online at: https://www.frontiersin.org/articles/10.3389/feart.2019.00087/full#supplementary-material

FIGURE S1 | Quantile–quantile plots which compares a theoretical quantiles of a (normal) density distribution with the observed quantile distribution, in order to assess whether the density distribution of the four studied intervals follows normality. Note, that all four time windows are characterized by heavy-tailed distributions.

TABLE S1 | The Neogene–Quaternary carbon isotope dataset. References to data sources included in the table.

TABLE S2 | The Permian–Triassic carbon isotope dataset. References to data sources included in the table.

TABLE S3 | The Ediacaran carbon isotope dataset. References to data sources included in the table.

TABLE S4 | The "Precambrian marine carbonate isotope database: Version 1.1" (or PMCID) (Shields and Veizer, 2002). Labels of columns have been altered for convenience during data processing.

REFERENCES

Adkins, J. F., Boyle, E. A., Curry, W. B., and Lutringer, A. (2003). Stable isotopes in deep-sea corals and a new mechanism for "vital effects". *Geochim. Cosmochim. Acta* 67, 1129–1143. doi: 10.1016/S0016-7037(00)01203-6

Allwood, A. C., Rosing, M. T., Flannery, D. T., Hurowitz, J. A., and Heirwegh, C. M. (2018). Reassessing evidence of life in 3,700-million-year-old rocks of Greenland. *Nature* 563, 241–244. doi: 10.1038/s41586-018-0610-4

Allwood, A. C., Walter, M. R., Kamber, B. S., Marshall, C. P., and Burch, I. W. (2006). Stromatolite reef from the early Archaean era of Australia. *Nature* 441, 714–718. doi: 10.1038/nature04764

Andres, M. S., Sumner, D. Y., Reid, R. P., and Swart, P. K. (2006). Isotopic fingerprints of microbial respiration in aragonite from Bahamian stromatolites. *Geology* 34, 973–976. doi: 10.1130/G22859A.1

Arp, G., Reimer, A., and Reitner, J. (2001). Photosynthesis-induced biofilm calcification and calcium concentrations in phanerozoic oceans. *Science* 292, 1701–1704. doi: 10.1126/science.1057204

Arp, G., Reimer, A., and Reitner, J. (2003). Microbialite formation in seawater of increased alkalinity, Satonda Crater Lake, Indonesia. *J. Sediment. Res.* 73, 105–127. doi: 10.1306/071002730105

Arp, G., Thiel, V., Reimer, A., Michaelis, W., and Reitner, J. (1999). Biofilm exopolymers control microbialite formation at thermal springs discharging into the alkaline Pyramid Lake, Nevada, USA. *Sediment. Geol.* 126, 159–176. doi: 10.1016/S0037-0738(99)00038-X

Arthur, M. A. (2000). "Volcanic contributions to the carbon and sulfur geochemical cycles and global change", in *Encyclopedia of Volcanoes (Elsevier)*, eds H. Sigurdsson, B. Houghton, H. Rymer, J. Stix, and S. McNutt (San Diego: Academic Press), 1045–1056.

Arthur, M. A., Dean, W. E., and Pratt, L. M. (1988). Geochemical and climatic effects of increased marine organic carbon burial at the Cenomanian/Turonian boundary. *Nature* 335, 714–717. doi: 10.1038/335714a0

Auclair, A. C., Joachimski, M. M., and Lécuyer, C. (2003). Deciphering kinetic, metabolic and environmental controls on stable isotope fractionations between seawater and the shell of *Terebratalia transversa* (Brachiopoda). *Chem. Geol.* 202, 59–78. doi: 10.1016/S0009-2541(03)00233-X

Auguie, B. (2017). *gridExtra: Miscellaneous Functions for "Grid" Graphics. R package version 2.3*. Available at: https://cran.r-project.org/package=gridExtra (accessed April 9, 2019).

Awramik, S. M. (1971). Precambrian columnar stromatolite diversity: reflection of metazoan appearance. *Science* 174, 825–827. doi: 10.1126/science.174.4011.825

Bachan, A., Lau, K. V., Saltzman, M. R., Thomas, E., Kump, L. R., and Payne, J. L. (2017). A model for the decrease in amplitude of carbon isotope excursions across the phanerozoic. *Am. J. Sci.* 317, 641–676. doi: 10.2475/06.2017.01

Bade, D. L., Carpenter, S. R., Cole, J. J., Hanson, P. C., and Hesslein, R. H. (2004). Controls of δ^{13}C-DIC in lakes: geochemistry, lake metabolism, and morphometry. *Limnol. Oceanogr.* 49, 1160–1172. doi: 10.4319/lo.2004.49.4.1160

Banner, J. L., and Hanson, G. N. (1990). Calculation of simultaneous isotopic and trace element variations during water-rock interaction with applications to carbonate diagenesis. *Geochim. Cosmochim. Acta* 54, 3123–3137. doi: 10.1016/0016-7037(90)90128-8

Barrell, J. (1917). Rhythms and measurement of geologic time. *Bull. Geol. Soc. Am.* 28, 745–904.

Bartley, J. K., and Kah, L. C. (2004). Marine carbon reservoir, Corg-Ccarb coupling, and the evolution of the Proterozoic carbon cycle. *Geology* 32, 129–132. doi: 10.1130/G19939.1

Baud, A., Cirilli, S., and Marcoux, J. (1997). Biotic response to mas extinction: the lowermost Triassic microbialites. *Facies* 36, 238–242.

Benzerara, K., Skouri-Panet, F., Li, J., Ferard, C., Gugger, M., Laurent, T., et al. (2014). Intracellular Ca-carbonate biomineralization is widespread in cyanobacteria. *Proc. Natl. Acad. Sci. U.S.A.* 111, 10933–10938. doi: 10.1073/pnas.1403510111

Bernard, S., Daval, D., Ackerer, P., Pont, S., and Meibom, A. (2017). Burial-induced oxygen-isotope re-equilibration of fossil foraminifera explains ocean paleotemperature paradoxes. *Nat. Commun.* 8:1134. doi: 10.1038/s41467-017-01225-9

Berner, R. A., Scott, M. R., and Thomlinson, C. (1970). Carbonate alkalinity in the pore waters of anoxic marine sediments. *Limnol. Oceanogr.* 15, 544–549. doi: 10.4319/lo.1970.15.4.0544

Birgel, D., Meister, P., Lundberg, R., Horath, T. D., Bontognali, T. R. R., Bahniuk, A. M., et al. (2015). Methanogenesis produces strong ^{13}C enrichment in stromatolites of Lagoa Salgada, Brazil: a modern analogue for Palaeo-/Neoproterozoic stromatolites? *Geobiology* 13, 245–266. doi: 10.1111/gbi.12130

Blair, N., Leu, A., Muñoz, E., Olsen, J., Kwong, E., and Des Marais, D. (1985). Carbon isotopic fractionation in heterotrophic microbial metabolism. *Appl. Environ. Microbiol.* 50, 996–1001.

Blamart, D., Rollion-bard, C., Cuif, J. P., Juillet-Leclerc, A., Lutringer, A., Van Weering, T. C. E., et al. (2005). "C and O isotopes in a deep-sea coral (*Lophelia pertusa*) related to skeletal microstructure," in *Cold-Water Corals and Ecosystems*, eds A. Freiwald and J. M. Roberts (Berlin: Springer-Verlag), 1005–1020. doi: 10.1007/3-540-27673-4_50

Brand, U., and Veizer, J. (1981). Chemical diagenesis of a multicomponent carbonate system -2: stable isotopes. *J. Sediment. Petrol.* 51, 987–997. doi: 10.1306/212F7DF6-2B24-11D7-8648000102C1865D

Bristow, T. F., and Kennedy, M. J. (2008). Carbon isotope excursions and the oxidant budget of the Ediacaran atmosphere and ocean. *Geology* 36, 863–866. doi: 10.1130/G24968A.1

Bundeleva, I. A., Shirokova, L. S., Pokrovsky, O. S., Bénézeth, P., Ménez, B., Gérard, E., et al. (2014). Experimental modeling of calcium carbonate precipitation by cyanobacterium *Gloeocapsa* sp. *Chem. Geol.* 374–375, 44–60. doi: 10.1016/j.chemgeo.2014.03.007

Busenberg, E., and Plummer, L. N. (1989). Thermodynamics of magnesian calcite solid-solutions at 25°C and 1 atm total pressure. *Geochim. Cosmochim. Acta* 53, 1189–1208. doi: 10.1016/0016-7037(89)90056-2

Butterfield, N. J. (2007). Macroevolution and macroecology through deep time. *Palaeontology* 50, 41–55. doi: 10.1111/j.1475-4983.2006.00613.x

Butterfield, N. J. (2009). Macroevolutionary turnover through the Ediacaran transition: ecological and biogeochemical implications. *Geol. Soc. Spec. Publ.* 326, 55–66. doi: 10.1144/sp326.3

Butterfield, N. J. (2018). Oxygen, animals and aquatic bioturbation: an updated account. *Geobiology* 16, 3–16. doi: 10.1111/gbi.12267

Caldeira, K., and Wickett, M. E. (2003). Anthropogenic carbon and ocean pH. *Nature* 425:365. doi: 10.1038/425365a

Canfield, D. E., and Farquhar, J. (2009). Animal evolution, bioturbation, and the sulfate concentration of the oceans. *Proc. Natl. Acad. Sci. U.S.A.* 106, 8123–8127. doi: 10.1073/pnas.0902037106

Corfield, R., and Cartlidge, J. E. (1993). "Oxygen and carbon isotope stratigraphy of the middle miocene, holes 805B and 806B," in *Proceedings of the Ocean Drilling Program, 130 Scientific Results*, Vol. 130, (College Station, TX), 307–322. doi: 10.2973/odp.proc.sr.130.026.1993

Cui, H., Kaufman, A. J., Xiao, S., Zhou, C., and Liu, X. M. (2017). Was the Ediacaran Shuram Excursion a globally synchronized early diagenetic event? Insights from methane-derived authigenic carbonates in the uppermost Doushantuo Formation, South China. *Chem. Geol.* 450, 59–80. doi: 10.1016/j.chemgeo.2016.12.010

Darroch, S. A., Smith, E. F., Laflamme, M., and Erwin, D. H. (2018). Ediacaran extinction and Cambrian explosion. *Trends Ecol. Evol.* 33, 653–663. doi: 10.1016/j.tree.2018.06.003

Derry, L. A., and France-Lanord, C. (1996). Neogene growth of the sedimentary organic carbon reservoir. *Paleoceanography* 11, 267–275. doi: 10.1029/95PA03839

Des Marais, D. J., and Canfield, D. E. (1994). "The carbon isotope biogeochemistry of microbial mats," in *Proceedings of the NATO Advanced Research Workshop on Structure, Development and Environmental Significance of Microbial Mats*, Vol. 35, (Berlin: Springer). doi: 10.1007/978-3-642-78991-5_30

D'Hondt, S., Donaghay, P., Zachos, J. C., Luttenberg, D., and Lindinger, M. (1998). Organic carbon fluxes and ecological recovery from the cretaceous-tertiary mass extinction. *Science* 282, 276–279. doi: 10.1126/science.282.5387.276

Dickens, G. R., O'Neil, J. R., Rea, D. K., and Owen, R. M. (1995). Dissociation of oceanic methane hydrate as a cause of the carbon isotope excursion at the end of the Paleocene. *Paleoceanography* 10, 965–971. doi: 10.1029/95PA02087

Dott, R. H. (1983). Episodic sedimentation—how normal is average? How rare is rare? Does it matter? *J. Sediment. Petrol.* 53, 5–23. doi: 10.1306/212F8148-2B24-11D7-8648000102C1865D

Dupraz, C., and Visscher, P. T. (2005). Microbial lithification in marine stromatolites and hypersaline mats. *Trends Microbiol.* 13, 429–438. doi: 10.1016/j.tim.2005.07.008

Emrich, K., Ehhalt, D. H., and Vogel, J. C. (1970). Carbon isotope fractionation during the precipitation of calcium carbonate. *Earth Planet. Sci. Lett.* 8, 363–371. doi: 10.1016/0012-821X(70)90109-3

Evans, D. A., Beukes, N. J., and Kirschvink, J. L. (1997). Low-latitude glaciation in the Palaeoproterozoic era. *Nature* 386, 262–266. doi: 10.1038/386262a0

Evans, D. A. D. (2000). Stratigraphic, geochronological, and paleomagnetic constraints upon the Neoproterozoic climatic paradox. *Am. J. Sci.* 300, 347–433. doi: 10.2475/ajs.300.5.347

Fantle, M. S., and DePaolo, D. J. (2006). Sr isotopes and pore fluid chemistry in carbonate sediment of the Ontong Java Plateau: calcite recrystallization rates and evidence for a rapid rise in seawater Mg over the last 10 million years. *Geochim. Cosmochim. Acta* 70, 3883–3904. doi: 10.1016/j.gca.2006.06.009

Fantle, M. S., and DePaolo, D. J. (2007). Ca isotopes in carbonate sediment and pore fluid from ODP Site 807A: the Ca^{2+}(aq)-calcite equilibrium fractionation factor and calcite recrystallization rates in Pleistocene sediments. *Geochim. Cosmochim. Acta* 71, 2524–2546. doi: 10.1016/j.gca.2007.03.006

Farquhar, G. D., Ehleringer, J. R., and Hubick, K. T. (1989). Carbon isotope discrimination and photosynthesis. *Annu. Rev. Plant Physiol. Plant Mol. Biol.* 40, 503–537. doi: 10.1146/annurev.pp.40.060189.002443

Fike, D. A., Gammon, C. L., Ziebis, W., and Orphan, V. J. (2008). Micron-scale mapping of sulfur cycling across the oxycline of a cyanobacterial mat: a paired nanoSIMS and CARD-FISH approach. *ISME J.* 2, 749–759. doi: 10.1038/ismej.2008.39

Folk, R. L. (1993). SEM imaging of bacteria and nannobacteria in carbonate sediments and rocks. *J. Sediment. Petrol.* 63, 990–999.

Fontanier, C., Jorissen, F. J., Michel, E., Cortijo, E., Vidal, L., and Anschutz, P. (2008). Stable oxygen and carbon isotopes of live (Stained) benthic foraminifera

from cap-ferret canyon (Bay of Biscay). *J. Foraminifer. Res.* 38, 39–51. doi: 10.2113/gsjfr.38.1.39

Fontanier, C., MacKensen, A., Jorissen, F. J., Anschutz, P., Licari, L., and Griveaud, C. (2006). Stable oxygen and carbon isotopes of live benthic foraminifera from the Bay of Biscay: microhabitat impact and seasonal variability. *Mar. Micropaleontol.* 58, 159–183. doi: 10.1016/j.marmicro.2005.09.004

Gagolewski, M. (2019). *R package stringi: Character String Processing Facilities*. Available at: http://www.gagolewski.com/software/stringi/ (accessed April 9, 2019).

Galbraith, E. D., Kwon, E. Y., Bianchi, D., Hain, M. P., and Sarmiento, J. L. (2015). The impact of atmospheric pCO_2 on carbon isotope ratios of the atmosphere and ocean. *Glob. Biogeochem. Cycles* 29, 307–324. doi: 10.1002/2014GB004929

Garrels, R. M., and Lerman, A. (1981). Phanerozoic cycles of sedimentary carbon and sulfur. *Proc. Natl. Acad. Sci. U.S.A.* 78, 4652–4656. doi: 10.1073/pnas.78.8.4652

Gattuso, J.-P., Epitalon, J.-M., Lavigne, H., and Orr, J. (2019). *seacarb: Seawater Carbonate Chemistry. R package version 3.2.11*. Available at: https://cran.r-project.org/package=seacarb (accessed April 9, 2019).

Ghaderi, A., Leda, L., Schobben, M., Korn, D., and Ashouri, A. R. (2014). High-resolution stratigraphy of the Changhsingian (Late Permian) successions of NW Iran and the Transcaucasus based on lithological features, conodonts and ammonoids. *Foss. Rec.* 17, 41–57. doi: 10.5194/fr-17-41-2014

Glunk, C., Dupraz, C., Beaissant, O., Gallagher, K. L., Verrechia, E. P., and Visscher, P. T. (2010). Microbially mediated carbonate precipitation in a hypersaline lake, Big Pond (Eleuthera, Bahamas). *Sedimentology* 58, 720–736. doi: 10.1111/j.1365-3091.2010.01180.x

Grant, S. (1990). Shell structure and distribution of Cloudina, a potential index fossil for the terminal Proterozoic. *Am. J. Sci.* 290, 261–294.

Gray, J. (1985). The microfossil record of early land plants: advances in understanding of early terrestrialization, 1970-1984. *Philos. Trans. R. Soc. Lond. B Biol. Sci.* 309, 167–195. doi: 10.1098/rstb.1985.0077

Grossman, E. L. (1984a). Carbon isotopic fractionation in live benthic foraminifera-comparison with inorganic precipitate studies. *Geochim. Cosmochim. Acta* 48, 1505–1512. doi: 10.1016/0016-7037(84)90406-X

Grossman, E. L. (1984b). Stable isotope fractionation in live benthic foraminifera from the southern California Borderland. *Palaeogeogr. Palaeoclimatol. Palaeoecol.* 47, 301–327. doi: 10.1016/0031-0182(84)90100-7

Grotzinger, J. P., Bowring, S. A., Saylor, B. Z., and Kaufman, A. J. (1995). Biostratigraphic and geochronologic constraints on early animal evolution. *Science* 270, 598–604. doi: 10.1126/science.270.5236.598

Grotzinger, J. P., Fike, D. A., and Fischer, W. W. (2011). Enigmatic origin of the largest-known carbon isotope excursion in Earth's history. *Nat. Geosci.* 4, 285–292. doi: 10.1038/ngeo1138

Grotzinger, J. P., and Knoll, A. H. (1999). Stromatolites in Precambrian carbonates: evolutionary mileposts or environmental dipsticks? *Annu. Rev. Earth Planet. Sci.* 27, 313–358. doi: 10.1146/annurev.earth.27.1.313

Grotzinger, J. P., and Rothman, D. H. (1996). An abiotic model for stromatolite morphogenesis. *Nature* 383, 423–425. doi: 10.1038/383423a0

Grotzinger, J. P., Watters, W. A., and Knoll, A. H. (2000). Calcified metazoans in thrombolite-stromatolite reefs of the terminal Proterozoic Nama Group, Namibia. *Paleobiology* 26, 334–359.

Guo, L., Andrews, J., Riding, R., Dennis, P., and Dresser, Q. (1996). Possible microbial effects on stable carbon isotopes in hot-spring travertines. *J. Sediment. Res.* 66, 468–473. doi: 10.1306/D4268379-2B26-11D7-8648000102C1865D

Hayes, J. M., Strauss, H., and Kaufman, A. J. (1999). The abundance of ^{13}C in marine organic matter and isotopic fractionation in the global biogeochemical cycle of carbon during the past 800 Ma. *Chem. Geol.* 161, 103–125. doi: 10.1016/S0009-2541(99)00083-2

Hazen, R. M., Papineau, D., Bleeker, W., Downs, R. T., Ferry, J. M., McCoy, T. J., et al. (2008). Mineral evolution. *Am. Mineral.* 93, 1693–1720. doi: 10.2138/am.2008.2955

Heindel, K., Birgel, D., Brunner, B., Thiel, V., Westphal, H., Gischler, E., et al. (2012). Post-glacial microbialite formation in coral reefs of the Pacific, Atlantic, and Indian Oceans. *Chem. Geol.* 304–305, 117–130. doi: 10.1016/j.chemgeo.2012.02.009

Heindel, K., Richoz, S., Birgel, D., Brandner, R., Klügel, A., Krystyn, L., et al. (2013). Biogeochemical formation of calyx-shaped carbonate crystal fans in the subsurface of the Early Triassic seafloor. *Gondwana Res.* 27, 840–861. doi: 10.1016/j.gr.2013.11.004

Holbourn, A., Kuhnt, W., Schulz, M., Flores, J. A., and Andersen, N. (2007). Orbitally-paced climate evolution during the middle Miocene "Monterey" carbon-isotope excursion. *Earth Planet. Sci. Lett.* 261, 534–550. doi: 10.1016/j.epsl.2007.07.026

Hönisch, B., Ridgwell, A., Schmidt, D. N., Thomas, E., Gibbs, S. J., Sluijs, A., et al. (2012). The geological record of ocean acidification. *Science* 335, 1058–1063. doi: 10.1126/science.1208277

Horodyski, R. J., and Knauth, L. P. (1994). Life on land in the precambrian. *Science* 263, 494–498. doi: 10.1126/science.263.5146.494

Hotinski, R. M., Bice, K. L., Kump, L. R., Najjar, R. G., and Arthur, M. A. (2001). Ocean stagnation and end-Permian anoxia. *Geology* 29, 7–10.

Hsü, K., and McKenzie, J. (1985). "A "Strangelove" ocean in the earliest tertiary," in *The Carbon Cycle and Atmospheric CO2: Natural Variations Archean to Present*, eds E. Sund-Quist and W. Broecker (Washington, DC: American Geophysical Union), 487–492. doi: 10.1029/GM032p0487

Irwin, H., Curtis, C., and Coleman, M. (1977). Isotopic evidence for source of diagenetic carbonates formed during burial of organic-rich sediments. *Nature* 269, 209–213. doi: 10.1038/269209a0

Jacobs, D. K., and Sahagian, D. L. (1993). Climate-induced fluctuations in sea level during non-glacial times. *Nature* 361, 710–712. doi: 10.1038/361710a0

Jahnke, R. A., and Jahnke, D. B. (2004). Calcium carbonate dissolution in deep sea sediments: reconciling microelectrode, pore water and benthic flux chamber results. *Geochim. Cosmochim. Acta* 68, 47–59. doi: 10.1016/S0016-7037(03)00260-6

Jimenez-Lopez, C., and Romanek, C. S. (2004). Precipitation kinetics and carbon isotope partitioning of inorganic siderite at 25°C and 1 atm. *Geochim. Cosmochim. Acta* 68, 557–571. doi: 10.1016/S0016-7037(03)00460-5

Knauth, L. P., and Kennedy, M. J. (2009). The late precambrian greening of the Earth. *Nature* 460, 728–732. doi: 10.1038/nature08213

Knoll, A. H. (2003). Biomineralization and evolutionary history. *Rev. Mineral. Geochem.* 54, 329–356. doi: 10.2113/0540329

Knoll, A. H., and Carroll, S. B. (1999). Early animal evolution: emerging views from comparative biology and geology. *Science* 284, 2129–2138.

Koohafkan, M. C. (2015). *kfigr: Integrated Code Chunk Anchoring and Referencing for R Markdown Documents. R package version 1.2*. Available at: https://cran.r-project.org/package=kfigr (accessed April 9, 2019).

Kristensen, E., Penha-Lopes, G., Delefosse, M., Valdemarsen, T., Quintana, C. O., and Banta, G. T. (2012). What is bioturbation? The need for a precise definition for fauna in aquatic sciences. *Mar. Ecol. Prog. Ser.* 446, 285–302. doi: 10.3354/meps09506

Kump, L. (1991). Interpreting carbon-isotope excursions: Strangelove oceans. *Geology* 19, 299–302.

Kump, L. R. (1989). Alternative modeling approaches to the geochemical cycles of carbon, sulfur, and strontium isotopes. *Am. J. Sci.* 289, 390–410. doi: 10.2475/ajs.289.4.390

Kump, L. R., and Arthur, M. A. (1999). Interpreting carbon-isotope excursions: carbonates and organic matter. *Chem. Geol.* 161, 181–198. doi: 10.1016/S0009-2541(99)00086-8

Kvenvolden, K. A. (2002). Methane hydrate in the global organic carbon cycle. *Terra Nova* 14, 302–306. doi: 10.1046/j.1365-3121.2002.00414.x

Leda, L., Korn, D., Ghaderi, A., Hairapetian, V., Struck, U., and Reimold, W. U. (2014). Lithostratigraphy and carbonate microfacies across the Permian–Triassic boundary near Julfa (NW Iran) and in the Baghuk Mountains (Central Iran). *Facies* 60, 295–325. doi: 10.1007/s10347-013-0366-0

Lepot, K., Benzerara, K., Brown, G. E., and Philippot, P. (2008). Microbially influenced formation of 2,724-million-year-old stromatolites. *Nat. Geosci.* 1, 118–121. doi: 10.1038/ngeo107

Logan, G., Hayes, J., Hieshima, G., and Summons, R. (1995). Terminal Proterozoic reorganization of biogeochemical cycles. *Nature* 376, 53–56. doi: 10.1038/376053a0

Mackenzie, F. T., and Andersson, A. J. (2011). "Biological control of diagenesis: influence of bacteria and relevance to ocean acidification," in *Encyclopedia of Geobiology*, eds J. Reitner and V. Thiel (Berlin: Springer), 137–143. doi: 10.1007/978-1-4020-9212-1_73

Marin, F., Corstjens, P., Gaulejac, B., de Vrind-De Jong, E., and Westbroek, P. (2000). Mucins and molluscan calcification. *J. Biol. Chem.* 275, 20667–20675. doi: 10.1074/jbc.M003006200

Marin, F., Smith, M., Isat, Y., Muyzert, G., and Westbroek, P. (1996). Skeletal matrices, muci, and the origin of invertebrate calcification. *Proc. Natl. Acad. Sci. U.S.A.* 93, 1554–1559. doi: 10.1073/pnas.93.4.1554

McConnaughey, T. A., and Whelan, J. F. (1997). Calcification generates protons for nutrient and bicarbonate uptake. *Earth Sci. Rev.* 42, 95–117. doi: 10.1016/S0012-8252(96)00036-0

McLoughlin, N., Wilson, L. A., and Brasier, M. D. (2008). Growth of synthetic stromatolites and wrinkle structures in the absence of microbes - Implications for the early fossil record. *Geobiology* 6, 95–105. doi: 10.1111/j.1472-4669.2007.00141.x

Mehra, A., and Maloof, A. (2018). Multiscale approach reveals that *Cloudina* aggregates are detritus and not in situ reef constructions. *Proc. Natl. Acad. Sci. U.S.A.* 115, E2519–E2527. doi: 10.1073/pnas.1719911115

Meister, P. (2013). Two opposing effects of sulfate reduction on carbonate precipitation in normal marine, hypersaline, and alkaline environments. *Geology* 41, 499–502. doi: 10.1130/G34185.1

Melim, L. A., Westphal, H., Swart, P. K., Eberli, G. P., and Munnecke, A. (2002). Questioning carbonate diagenetic paradigms: evidence from the Neogene of the Bahamas. *Mar. Geol.* 185, 27–53. doi: 10.1016/S0025-3227(01)00289-4

Merz, M. U. E. (1992). The biology of carbonate precipitation by cyanobacteria. *Facies* 26, 81–101. doi: 10.1007/BF02536920

Meyer, K. M., Ridgwell, A., and Payne, J. L. (2016). The influence of the biological pump on ocean chemistry: implications for long-term trends in marine redox chemistry, the global carbon cycle, and marine animal ecosystems. *Geobiology* 14, 207–219. doi: 10.1111/gbi.12176

Miller, K. G., Kominz, M. A., Browning, J. V., Wright, J. D., Mountain, G. S., Katz, M. E., et al. (2005). The phanerozoic record of global sea-level change. *Science* 310, 1293–1298. doi: 10.1126/science.1116412

Milliman, J. D., Troy, P. J., Balch, W. M., Adams, A. K., Li, Y. H., and Mackenzie, F. T. (1999). Biologically mediated dissolution of calcium carbonate above the chemical lysocline? *Deep Sea Res. Part I Oceanogr. Res. Pap.* 46, 1653–1669. doi: 10.1016/S0967-0637(99)00034-5

Mills, B. J. W., Batterman, S. A., and Field, K. J. (2018). Nutrient acquisition by symbiotic fungi governs Palaeozoic climate transition. *Philos. Trans. R. Soc. B Biol. Sci.* 373:20160503. doi: 10.1098/rstb.2016.0503

Muttoni, G., Gaetani, M., Kent, D., Sciunnach, D., Angiolini, L., Berra, F., et al. (2009). Opening of the Neo-tethys ocean and the Pangea B to Pangea A transformation during the Permian. *GeoArabia* 14, 17–48. doi: 10.1016/S0012-821X(03)00452-7

Nutman, A. P., Bennett, V. C., Friend, C. R. L., Van Kranendonk, M. J., and Chivas, A. R. (2016). Rapid emergence of life shown by discovery of 3,700-million-year-old microbial structures. *Nature* 537, 535–538. doi: 10.1038/nature19355

O'Leary, M. H. (1988). Carbon isotopes in photosynthesis. *Science* 38, 328–336.

Payne, J. L., Boyer, A. G., Brown, J. H., Finnegan, S., Kowalewski, M., Krause, R. A., et al. (2009). Two-phase increase in the maximum size of life over 3.5 billion years reflects biological innovation and environmental opportunity. *Proc. Natl. Acad. Sci. U.S.A.* 106, 24–27. doi: 10.1073/pnas.0806314106

Payne, J. L., Turchyn, A. V., Paytan, A., Depaolo, D. J., Lehrmann, D. J., Yu, M., et al. (2010). Calcium isotope constraints on the end-Permian mass extinction. *Proc. Natl. Acad. Sci. U.S.A.* 107, 8543–8548. doi: 10.1073/pnas.0914065107

Pentecost, A., and Franke, U. (2010). Photosynthesis and calcification of the stromatolitic freshwater cyanobacterium Rivularia. *Eur. J. Phycol.* 45, 345–353. doi: 10.1080/09670262.2010.492914

Pentecost, A., and Spiro, B. (1990). Stable carbon and oxygen isotope composition of calcites associated with modern freshwater cyanobacteria and algae. *Geomicrobiol. J.* 8, 17–26. doi: 10.1080/01490459009377875

Planavsky, N. J., Tarhan, L. G., Bellefroid, E. J., Evans, D. A. D., Reinhard, C. T., Love, G. D., et al. (2015). Late proterozoic transitions in climate, oxygen, and tectonics, and the rise of complex life. *Paleontol. Soc. Pap.* 21, 47–82. doi: 10.1017/S1089332600002965

Pope, M. C., and Grotzinger, J. P. (2000). Controls on fabric and morphology of tufas and stromatolites uppermost Pethei Group (1.8Ga), Great Sklave lake, Northwest Canada. *Soc. Sediment. Geol.* 67, 103–121.

Porter, S. M. (2010). Calcite and aragonite seas and the de novo acquisition of carbonate skeletons. *Geobiology* 8, 256–277. doi: 10.1111/j.1472-4669.2010.00246.x

Prokoph, A., Shields, G. A., and Veizer, J. (2008). Compilation and time-series analysis of a marine carbonate $\delta^{18}O$, $\delta^{13}C$, $^{87}Sr/^{86}Sr$ and $\delta^{34}S$ database through Earth history. *Earth Sci. Rev.* 87, 113–133. doi: 10.1016/j.earscirev.2007.12.003

R Core Team (2018). *R: A Language and Environment for Statistical Computing*. Vienna: R Foundation for Statistical Computing.

Rampino, M. R., and Caldeira, K. (2005). Major perturbation of ocean chemistry and a 'Strangelove Ocean' after the end-Permian mass extinction. *Terra Nova* 17, 554–559. doi: 10.1111/j.1365-3121.2005.00648.x

Rau, G., Riebesell, U., and Wolf-Gladrow, D. (1997). CO_{2aq}-dependent photosynthetic ^{13}C fractionation in the ocean: a model versus measurements. *Glob. Biogeochem. Cycles* 11, 267–278. doi: 10.1029/97GB00328

Reitner, J. (1993). Modern cryptic microbialite/metazoan facies from lizard island (great barrier reef, Australia) formation and concepts. *Facies* 29, 3–40. doi: 10.1007/BF02536915

Reitner, J., Peckmann, J., Reimer, A., Schumann, G., and Thiel, V. (2005). Methane-derived carbonate build-ups and associated microbial communities at cold seeps on the lower Crimean shelf (Black Sea). *Facies* 51, 66–79. doi: 10.1007/s10347-005-0059-4

Renne, P. R., Black, M. T., Zichao, Z., Richards, M. A., and Basu, A. R. (1995). Synchrony and causal relations between Permian-Triassic boundary crises and siberian flood volcanism. *Science* 269, 1413–1416. doi: 10.1126/science.269.5229.1413

Ridgwell, A. (2005). A Mid Mesozoic Revolution in the regulation of ocean chemistry. *Mar. Geol.* 217, 339–357. doi: 10.1016/j.margeo.2004.10.036

Riding, R. (2000). Microbial carbonates: the geological record of calcified bacterial-algal mats and biofilms. *Sedimentology* 47, 179–214. doi: 10.1046/j.1365-3091.2000.00003.x

Romanek, C. S., Grossman, E. L., and Morse, J. W. (1992). Carbon isotopic fractionation in synthetic aragonite and calcite: effects of temperature and precipitation rate. *Geochim. Cosmochim. Acta* 56, 419–430. doi: 10.1016/0016-7037(92)90142-6

Rothman, D. H., Hayes, J. M., and Summons, R. E. (2003). Dynamics of the Neoproterozoic carbon cycle. *Proc. Natl. Acad. Sci. U.S.A.* 100, 8124–8129. doi: 10.1073/pnas.0832439100

Rubinson, M., and Clayton, R. N. (1969). Carbon-13 fractionation between aragonite and calcite. *Geochim. Cosmochim. Acta* 33, 997–1002. doi: 10.1016/0016-7037(69)90109-4

Ruhl, M., Bonis, N. R., Reichart, G.-J., Sinninghe Damsté, J. S., and Kürschner, W. M. (2011). Atmospheric carbon injection linked to end-triassic mass extinction. *Science* 333, 430–434. doi: 10.1126/science.1204255

Sadler, P. M. (1981). Sediment accumulation rates and the completeness of stratigraphic sections. *J. Geol.* 89, 569–584. doi: 10.1086/628623

Sánchez-Román, M., Fernández-Remolar, D., Amils, R., Sánchez-Navas, A., Schmid, T., Martin-Uriz, P. S., et al. (2014). Microbial mediated formation of Fe-carbonate minerals under extreme acidic conditions. *Sci. Rep.* 4:4767. doi: 10.1038/srep04767

Sánchez-Román, M., Vasconcelos, C., Schmid, T., Dittrich, M., McKenzie, J. A., Zenobi, R., et al. (2008). Aerobic microbial dolomite at the nanometer scale: implications for the geologic record. *Geology* 36, 879–882. doi: 10.1130/G25013A.1

Sarmiento, J. L., and Gruber, N. (2004). *Calcium Carbonate Cycling, in Ocean Biogeochemical Dynamics*. New York, NY: Princeton University Press, 1–44. doi: 10.2307/j.ctt3fgxqx

Schidlowski, M., Gorzawski, H., and Dor, I. (1994). Carbon isotope variations in a solar pond microbial mat: role of environmental gradients as steering variables. *Geochim. Cosmochim. Acta* 58, 2289–2298. doi: 10.1016/0016-7037(94)90011-6

Schobben, M., Ullmann, C. V., Leda, L., Korn, D., Struck, U., Reimold, W. U., et al. (2016). Discerning primary versus diagenetic signals in carbonate carbon and oxygen isotope records: an example from the Permian–Triassic boundary of Iran. *Chem. Geol.* 422, 94–107. doi: 10.1016/j.chemgeo.2015.12.013

Schobben, M., van de Velde, S., Gliwa, J., Leda, L., Korn, D., Struck, U., et al. (2017). Latest Permian carbonate-carbon isotope variability traces heterogeneous organic carbon accumulation and authigenic carbonate formation. *Clim. Past* 13, 1635–1659. doi: 10.5194/cp-2017-66

Scholle, P. A., and Arthur, M. A. (1980). Carbon isotope fluctuations in Cretaceous pelagic limestones: potential stratigraphic and petroleum exploration tool. *Am. Assoc. Pet. Geol. Bull.* 64, 67–87.

Schrag, D. P., Higgins, J. A., Macdonald, F. A., and Johnston, D. T. (2013). Authigenic carbonate and the history of the global carbon cycle. *Science* 339, 540–543. doi: 10.1126/science.1229578

Sforna, M. C., Daye, M., Philippot, P., Somogyi, A., van Zuilen, M. A., Medjoubi, K., et al. (2017). Patterns of metal distribution in hypersaline microbialites during early diagenesis: implications for the fossil record. *Geobiology* 15, 259–279. doi: 10.1111/gbi.12218

Shackleton, N., and Hall, M. (1984). Carbon isotope data from Leg 74 sediments. *Initial Rep. Deep Sea Drill. Proj.* 74, 613–619. doi: 10.2973/dsdp.proc.74.116.1984

Shields, G., and Veizer, J. (2002). The Precambrian marine carbonate isotope database: version 1.1. *Geochem. Geophys. Geosyst.* 3, 1–12. doi: 10.1029/2001GC000266

Shields, G. A. (2017). Earth system transition during the Tonian–Cambrian interval of biological innovation: nutrients, climate, oxygen and the marine organic carbon capacitor. *Geol. Soc. Lond. Spec. Publ.* 448, 161–177. doi: 10.1144/SP448.17

Skinner, H. C. W., and Jahren, A. H. (2003). "Biomineralization," in *Treatise on Geochemistry*, eds W. H. Schlesinger, H. D. Holland, and K. K. Turekian (Oxford: Pergamon), 682. doi: 10.1016/B0-08-043751-6/08128-7

Soetaert, K., and Petzoldt, T. (2018). *marelac: Tools for Aquatic Sciences. R package version 2.1.9*. Available at: https://cran.r-project.org/package=marelac (accessed April 9, 2019).

Soetaert, K., Petzoldt, T., and Setzer, R. (2010). Package deSolve: solving initial value differential equations in R. *J. Stat. Softw.* 33, 1–25. doi: 10.18637/jss.v033.i09

Sommerfield, C. K. (2006). On sediment accumulation rates and stratigraphic completeness: lessons from Holocene ocean margins. *Cont. Shelf Res.* 26, 2225–2240. doi: 10.1016/j.csr.2006.07.015

Spero, H., and Williams, D. (1988). Extracting environmental information from planktonic foraminiferal δ13C data. *Nature* 335, 717–719. doi: 10.1038/335717a0

Swart, P. K. (2008). Global synchronous changes in the carbon isotopic composition of carbonate sediments unrelated to changes in the global carbon cycle. *Proc. Natl. Acad. Sci. U.S.A.* 105, 13741–13745. doi: 10.1073/pnas.0802841105

Tarhan, L. G., Droser, M. L., Planavsky, N. J., and Johnston, D. T. (2015). Protracted development of bioturbation through the early Palaeozoic Era. *Nat. Geosci.* 8, 865–869. doi: 10.1038/ngeo2537

Thompson, J. B., and Ferris, F. G. (1992). Cyanobacterial precipitation of gypsum, calcite and magnesitre from natural lake water. *Geology* 18, 995–998.

Tyrrell, T., and Zeebe, R. E. (2004). History of carbonate ion concentration over the last 100 million years. *Geochim. Cosmochim. Acta* 68, 3521–3530. doi: 10.1016/j.gca.2004.02.018

Urey, H. C. (1947). The thermodynamic properties of isotopic substances. *J. Chem. Soc.* 562–581.

Valentine, J. W., Jablonski, D., and Erwin, D. H. (1999). Fossils, molecules and embryos: new perspectives on the Cambrian explosion. *Development* 126, 851–859.

Vasconcelos, C., McKenzie, J. A., Bernasconi, S., Grujic, D., and Tien, A. J. (1995). Microbial mediation as a possible mechanism for natural dolomite formation at low temperature. *Nature* 377, 220–222. doi: 10.1038/377220a0

Vasconcelos, C., Warthmann, R., McKenzie, J. A., Visscher, P. T., Bittermann, A. G., and van Lith, Y. (2006). Lithifying microbial mats in Lagoa Vermelha, Brazil: modern precambrian relics? *Sediment. Geol.* 185, 175–183. doi: 10.1016/j.sedgeo.2005.12.022

Vaziri, S. H., Majidifard, M. R., and Laflamme, M. (2018). Diverse assemblage of ediacaran fossils from central Iran. *Sci. Rep.* 8:5060. doi: 10.1038/s41598-018-23442-y

Veizer, J., Ala, D., Azmy, K., Bruckschen, P., Buhl, D., Bruhn, F., et al. (1999). 87Sr/86Sr, 13C and 18O evolution of Phanerozoic seawater. *Chem. Geol.* 161, 59–88. doi: 10.1016/S0009-2541(99)00081-9

Vermeij, G. J. (1977). The Mesozoic marine revolution: evidence from snails, predators and grazers. *Paleobiology* 3, 245–258.

Vincent, E., and Berger, W. (1985). "Carbon dioxide and polar cooling in the miocene: the Monterey hypothesis," in *The Carbon Cycle and Atmospheric CO2: Natural Variations Archean to Present*, eds E. Broecker and W. Sundquist (Washington, DC: American Geophysical Union), 455–468. doi: 10.1029/GM032p0455

Visscher, P. T., Reid, P. R., and Bebout, B. M. (2000). Microscale observations of sulfate reduction: correlation of microbial activity with lithified micritic laminae in modern marine stromatolites. *Geology* 28, 919–922.

Visscher, P. T., and Stolz, J. F. (2005). Microbial mats as bioreactors: populations, processes, and products. *Palaeogeogr. Palaeoclimatol. Palaeoecol.* 219, 87–100. doi: 10.1016/j.palaeo.2004.10.016

Walter, M. R., and Heys, G. R. (1985). Links between the rise of metazoa and the decline of stromatolites. *Precambrian Res.* 29, 149–174. doi: 10.1016/0301-9268(85)90066-X

Webb, G. E. (1996). Was Phanerozoic reef history controlled by the distribution of non-enzymatically secreted reef carbonates (microbial carbonate and biologically induced cement)? *Sedimentology* 43, 947–971. doi: 10.1111/j.1365-3091.1996.tb01513.x

Wellman, C. H., Osterloff, P. L., and Mohiuddin, U. (2003). Fragments of the earliest land plants. *Nature* 425, 282–285. doi: 10.1038/nature01884

Westbroek, P., and Marin, F. (1998). A marriage of bone and nacre. *Nature* 392, 861–862. doi: 10.1038/31798

Wickham, H. (2009). *ggplot2: Elegant Graphics for Data Analysis*. New York, NY: Springer-Verlag.

Wickham, H. (2016). *gtable: Arrange 'Grobs' in Tables. R package version 0.2.0*. Available at: https://CRAN.R-project.org/package=gtable (accessed April 9, 2019).

Wickham, H., François, R., Henry, L., and Müller, K. (2018). *dplyr: A Grammar of Data Manipulation. R package version 0.7.8*. Available at: https://cran.r-project.org/package=dplyr (accessed April 9, 2019).

Wickham, H., and Henry, L. (2018). *tidyr: Easily Tidy Data with 'spread()' and 'gather()' Functions. R package version 0.8.2*. Available at: https://CRAN.R-project.org/package=tidyr (accessed April 9, 2019).

Wignall, P. B., and Twitchett, R. J. (1996). Oceanic anoxia and the End Permian mass extinction. *Science* 272, 1155–1158. doi: 10.1126/science.272.5265.1155

Wood, R. A., Grotzinger, J. P., and Dickson, J. A. (2002). Proterozoic modular biomineralized metazoan from the Nama Group, Namibia. *Science* 296, 2383–2386. doi: 10.1126/science.1071599

Xie, Y. (2014). "knitr: a comprehensive tool for reproducible research in R," in *Implementing Reproducible Computational Research*, eds V. Stodden, F. Leisch, and R. D. Peng (Boca Raton, FL: Chapman).

Xie, Y. (2015). *Dynamic Documents with {R} and knitr*, 2nd Edn. Boca Raton, FL: Chapman.

Xie, Y. (2018). *knitr: A General-Purpose Package for Dynamic Report Generation in R. R package version 1.21*. Available at: https://yihui.name/knitr/ (accessed April 9, 2019).

Zachos, J., Pagani, M., Sloan, L., Thomas, E., and Billups, K. (2001). Trends, rhythms, and aberrations in global climate 65 Ma to present. *Science* 292, 686–693. doi: 10.1126/science.1059412

Zeebe, R. E., and Westbroek, P. (2003). A simple model for the $CaCO_3$ saturation state of the ocean; the "Strangelove," the "Neritan," and the "Cretan" ocean. *Geochem. Geophys. Geosyst.* 4:26. doi: 10.1029/2003GC000538

Zhang, J., Quay, P. D., and Wilbur, D. O. (1995). Carbon isotope fractionation during gas-water exchange and dissolution of CO_2. *Geochim. Cosmochim. Acta* 59, 107–114. doi: 10.1016/0016-7037(95)91550-D

Zhang, R., Follows, M. J., Grotzinger, J. P., and Marshall, J. (2001). Could the Late Permian deep ocean have been anoxic? *Paleoceanography* 16, 317–329.

Zhu, M., Zhang, J., and Yang, A. (2007). Integrated Ediacaran (Sinian) chronostratigraphy of South China. *Palaeogeogr. Palaeoclimatol. Palaeoecol.* 254, 7–61. doi: 10.1016/j.palaeo.2007.03.025

Conflict of Interest Statement: The authors declare that the research was conducted in the absence of any commercial or financial relationships that could be construed as a potential conflict of interest.